INL/EXT-09-17197

ATR 2A/2B As-Run Neutronics Uncertainty Analysis

Hiroshi Sagara
Gray S. Chang

October 2009

The INL is a U.S. Department of Energy National Laboratory
operated by Battelle Energy Alliance

INL/EXT-09-17197

ATR 2A/2B As-Run Neutronics Uncertainty Analysis

Hiroshi Sagara
Gray S. Chang

October 2009

Idaho National Laboratory
Idaho Falls, Idaho 83415

http://www.inl.gov

Prepared for the
U.S. Department of Energy
Office of Nuclear Energy
Under DOE Idaho Operations Office
Contract DE-AC07-05ID14517

INL/EXT-09-17197

ATR 2A/2B As-Run Neutronics Uncertainty Analysis

Advanced Fuel Cycle Initiative

Prepared for
U.S. Department of Energy
Transmutation Fuels Campaign
Hiroshi Sagara, Gray S. Chang
Idaho National Laboratory
October 2009
AFCI-FUEL-FUEL-TD-RT-2009-000295

ABSTRACT

Neutronics calculations contain several uncertainties such as nuclear data, Monte-Carlo (MC) statistics deviation of the neutron flux tally, initial mass load, power history, etc. Minor Actinides (MAs) have shortage of measured nuclear data (cross-section, thermal property, etc.) and have large uncertainty based on nuclear data. We need to consider the uncertainty caused by nuclear data, especially to treat MA loaded fuel in future reactor designs, safety analysis, and irradiation testing of fuel for these reactors.

Uncertainty analysis relating to calculations for AFC-2A and AFC-2B has been performed. The methodology to treat the nuclear cross section covariance and global uncertainty in the depletion and buildup calculation were established by additions to the current MCWO code system with interface to the ORIGEN Library. This uncertainty analysis methodology was applied to AFC-2A and AFC-2B irradiation analysis, and uncertainties of HM density, elemental composition, isotope composition and burnup are calculated. As a result, the sensitivity of cross section errors are evaluated coupled with original as-run calculations by MCWO, and the importance of cross section error to the final output is evaluated by sensitivity analysis. This methodology and results can provide the productive information to PIE experimentalists to discuss the discrepancy between calculations and experiments in the AFCI program. Also, the uncertainty information can be utilized for the safety evaluation and validation of fuel burnup codes and nuclear data.

CONTENTS

FIGURES

TABLES

ACRONYMS

AFC	Advanced Fuel Cycle
ATR	Advanced Test Reactor
MAs	Minor-Actinides
EFPD	effective full-power days
EFT	East Flux Trap
INL	Idaho National Laboratory
JAEA	Japan Atomic Energy Agency
PWR	Pressurized water reactor
PIE	Post Irradiation Examination
HM	Heavy Metal
MC	Monte-Carlo
MCNP	Monte Carlo N-Particle (neutron and photon transport code)
MCWO	Monte Carlo with ORIGEN2 (neutron burnup analysis code)

ATR 2A/2B AS-RUN NEUTRONICS UNCERTAINTY ANALYSIS

1. INTRODUCTION

Neutronics calculations contain several uncertainties such as nuclear data, MC statistics deviation of neutron flux tally, initial mass load, power history, etc. MAs have shortage of measured nuclear data (cross-section, thermal property, etc.) and have a large uncertainty band on nuclear data as shown in Figure 1. We need to consider the uncertainty caused by nuclear data especially to treat MA including fuel in future reactor designs, safety analysis, irradiation test of fuel concepts for these future reactors, and so on.

Recently covariance matrixes of nuclear data have been included in ENDF/B1, JENDL2, JEF3, TENDL4 and Low-fidelity Covariance5. These contain covariance data of the cross sections for several important nuclides for elastic scattering, inelastic scattering, (n,2n) reactions, radioactive capture and fission (cross section and nubar), in which various approximations were utilized depending on the mass of the target, the neutron energy range, and the neutron reaction.

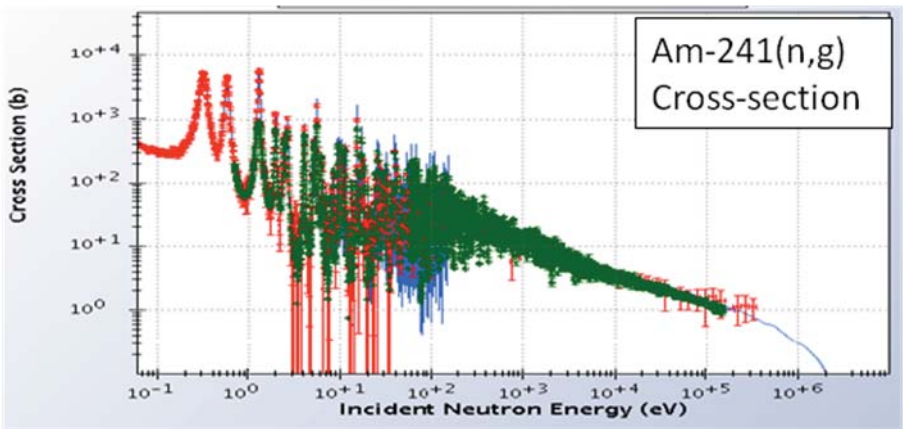

(a) Am-241 capture cross-section with measurement data (ENDF/VII)

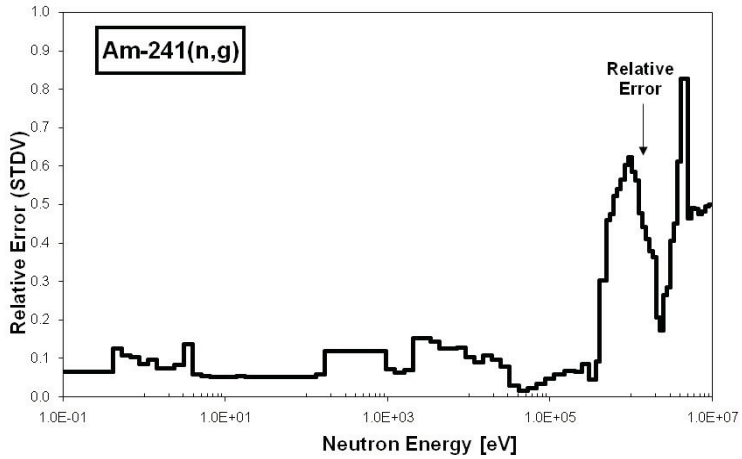

(b) Am-241 capture cross-section error

Figure 1. Am-241 capture cross-sections and its error.

1.1 Objectives

- To establish the method of uncertainty analysis for AFC-2A and -2B[6,7,8,9,10] irradiation tests
- To evaluate AFC-2A and -2B fuel depletion and buildup with error based on calculation uncertainty
- To provide the uncertainty information related to the neutronics calculation for PIE chemist to assess the difference between the measurement and calculation.

2. METHODOLOGY

2.1 Methodology of Uncertainty Analysis

The calculation flow chart is shown in Figure 2. In this work, we established the covariance matrix treatment to achieve effective cross-section error in the irradiated AFC-2A and -2B fuel pins, and the global uncertainty treatment in depletion calculation by ORIGEN2.2[11] and Bateman Equation. We can apply these methodologies to MCWO[12] code with interface to the ORIGEN Library. Detailed explanation of each calculation flow chart step is described in next paragraph.

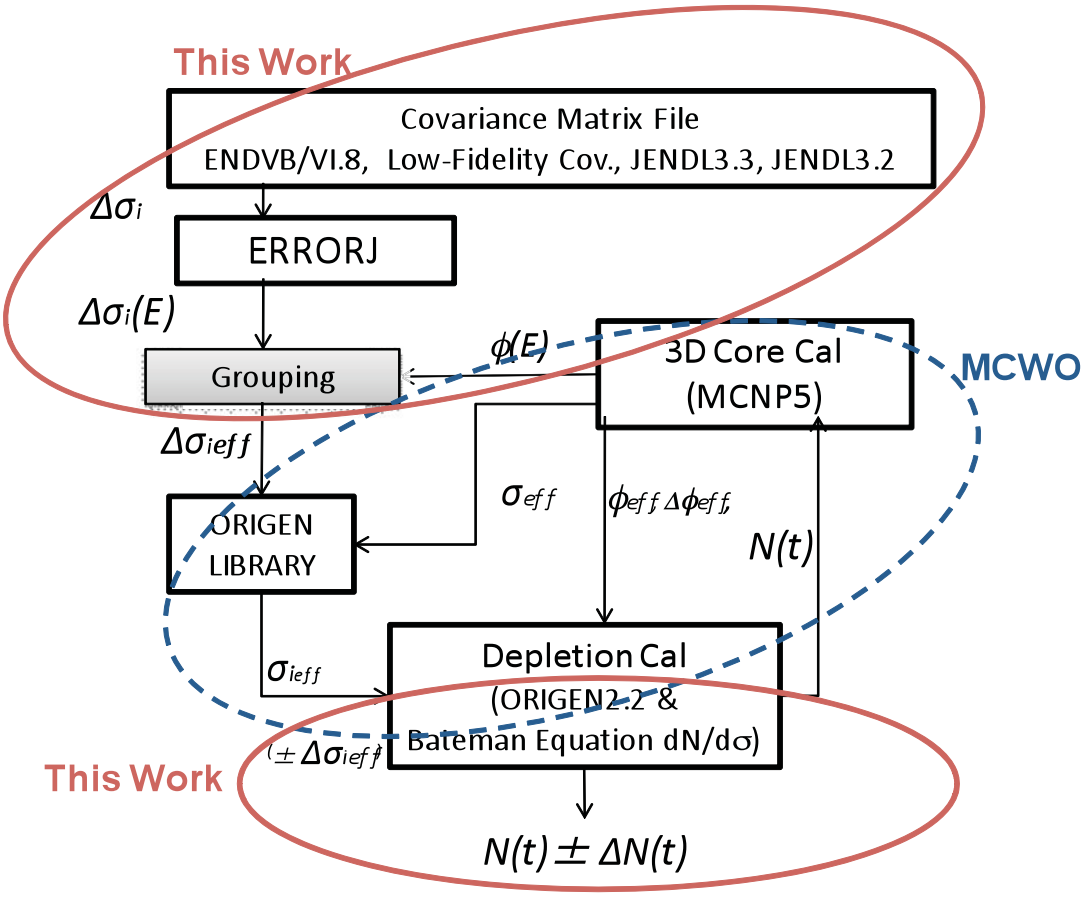

Figure 2. Flow chart of Uncertainty Analysis.

2.1.1 Cross-section uncertainty

When the uncertainties of the nuclear parameters are evaluated in a deterministic manner,

Covariances of the energy-averaged (multi-group) cross sections are necessary. In the present work, ERRORJ2.3 code is utilized for this purpose.

ERRORJ[13] is a processing code to transform cross section covariance given in the ENDF format into energy-averaged cross section covariance. ERRORJ can process the covariance data of cross sections including resonance parameters, and angular and energy distributions of secondary neutrons. The original ERRORJ code was developed by K. Kosako in 1999[14] based on the ERRORR module of the NJOY code,[15] to generate the covariance of multi-group cross sections from the covariance data given in the nuclear data files. ERRORJ can process the covariance of the cross sections including Breit-Wigner and Reich-Moore resonance parameters, angular and energy distributions of secondary neutrons and the number of neutrons generated by the fission reaction. ERRORJ can also process the covariance of the resonance parameters contained in the 'compact format' recently generated. ERRORJ had been the first code to process such covariance data in the world. Recently, the PUFF-IV[16] code has been developed at the Oak Ridge National Laboratory. The PUFF-IV code can process the covariance of all the resonance parameters, and it can read the covariance in the compact format. However, the PUFF-IV code cannot treat the covariance of angular and energy distributions of secondary neutrons.

By utilizing ERRORJ, the covariance matrix of each nuclide is converted to the user suggested energy group constants, and by weighting the AFC-2A and -2B neutron spectrum, the effective cross-section error in AFC irradiation fuel pins are created. In the present work, covariance matrixes are extracted from ENDF/VI.8, ENDF/VII, JENDL3.3 and Low-fidelity Covariance for Actinides (U-235, U-238, Pu-238, Pu-239, Pu-240, Pu-241, Pu-242, Np-237, Am-241, Am-243, and Cm-244).

Cross-section uncertainty of each nuclide reaction type is calculated by ERRORJ code with 216 energy groups with constant lethargy width. The effective one-group error of cross-section is calculated by

$$\overline{\Delta\sigma_{eff}} = \int \frac{\Delta\sigma(E)\phi(E)}{\phi(E)} dE \qquad \text{(Eq. 1)},$$

where $\phi(E)$ represents the energy dependent neutron flux in AFC-2A and -2B fuel pin position and $\Delta\sigma(E)$ is the energy dependent cross-section error provided by the output of ERRORJ.

2.1.2 Flux uncertainty

Since there is no measurement data of neutron flux absolute value in the current AFC-2A and -2B irradiation tests, MC statistical deviation is taken as the flux uncertainty in the full core calculation result provided by Dr. Gray Chang. The MC statistical deviation in the present work was very low (less than 0.5%) thus, much lower than cross-section uncertainty. For simplicity, the flux uncertainty is omitted in this work. The calculation with a boundary neutron source for AFC-2A and -2B irradiation position has also been performed and the flux uncertainty was input as 10% since difference between full core models in flux was 5 to 10% in AFC-2A and -2B irradiation position. The detailed table sets of these results are included in the Appendix A.

Other uncertainties such as initial load, and power history are not considered in the present report. As -built fuel information and as-run power history, provided by MCNP full core analyses, are utilized as fixed values. The unique phenomena of the metal fuel, swelling and elements migration during the irradiation, are also not considered in this work. The depletion and buildup results for each fuel pin are the average value for each pin.

Rare Earth (RE) depletion and buildup have cross section and fission yield errors. Though as-run depletion and buildup calculation of RE is not performed in this work, the important uncertainty data sets relating to cross section and fission yields are included in the Appendix B.

2.1.3 Global Uncertainty Analysis

In nuclear transmutation calculations, we need each nuclide uncertainty to be transported to the final nuclide uncertainty. To evaluate the global uncertainty in transmutation, depletion calculations can be performed using either a numerical approach, such as ORIGEN2.2, or by solving Bateman Equation with perturbation of each parameter.

The mono HM nuclide transmutation from nuclide 1 to nuclide m, the transmutation differential equation, is described with Bateman equation as follows:

$$\frac{dN_1(t)}{dt} = -\lambda_1 N_1(t)$$

$$\frac{dN_2(t)}{dt} = \lambda_i \cdot N_1(t) - \lambda_2 N_2(t)$$

$$\frac{dN_3(t)}{dt} = \lambda_{ii} \cdot N_2(t) - \lambda_3 \cdot N_3(t)$$

…

$$\frac{dN_m(t)}{dt} = \lambda_{m-i} \cdot N_{m-i}(t) - \lambda_m \cdot N_m(t) \qquad \text{(Eq. 2)}$$

where λ is a constant and consists of micro cross-section σ, neutron flux ϕ, and decay constant.

The integral solution of the differential equation is

$$N_m(t) = N_1^0 \cdot \prod_{a=i}^{m-i} \lambda_a \cdot \sum_{c=1}^{m} e^{-\lambda_c \cdot t} \prod_{c \neq d} \frac{1}{(\lambda_d - \lambda_c)}. \qquad \text{(Eq. 3)}$$

The increment difference of N_m(t) is described as following,

$$dN_m = \frac{\partial N_m}{\partial \sigma_{c1}} d\sigma_{c1} + \frac{\partial N_m}{\partial \sigma_{f1}} d\sigma_{f1} + \frac{\partial N_m}{\partial \sigma_{(n,2n)1}} d\sigma_{(n,2n)1} + ... + \frac{\partial N_m}{\partial \sigma_{(n,2n)m}} d\sigma_{(n,2n)m} + \frac{\partial N_m}{\partial \phi} d\phi \qquad \text{(Eq. 4)}$$

We assume that N_m(t) is the linear function with each parameter with a width of $\pm\Delta$, the equation can be converted to the following,

$$\Delta N_m = \sqrt{\left(\frac{\partial N_m}{\partial \sigma_{c1}} \Delta\sigma_{c1}\right)^2 + \left(\frac{\partial N_m}{\partial \sigma_{f1}} \Delta\sigma_{f1}\right)^2 + \left(\frac{\partial N_m}{\partial \sigma_{(n,2n)1}} \Delta\sigma_{(n,2n)1}\right)^2 ... + \left(\frac{\partial N_m}{\partial \phi} \Delta\phi\right)^2}. \qquad \text{(Eq. 5)}$$

With this equation, we can treat the transportation of each nuclide/reaction uncertainty to the final nuclide as global uncertainty. Depletion calculations can be performed using either a numerical approach such as ORIGEN2.2 or by solving Bateman Equation in Eq. 3, and Eq. 5 can be utilized to evaluate the global uncertainty of nuclide m.

To calculate the global uncertainty of each nuclide, the EFT irradiation position isolated model with boundary neutron source is applied. Though the isolated model has 5 to 10% discrepancy in the results of HM depletion and buildup from full core model, it provides good enough information for each differential coefficient in Eq.4 and a good uncertainty ratio. Finally the global uncertainties calculated by the isolated model are applied to the result of full core depletion and buildup calculation in ratio.

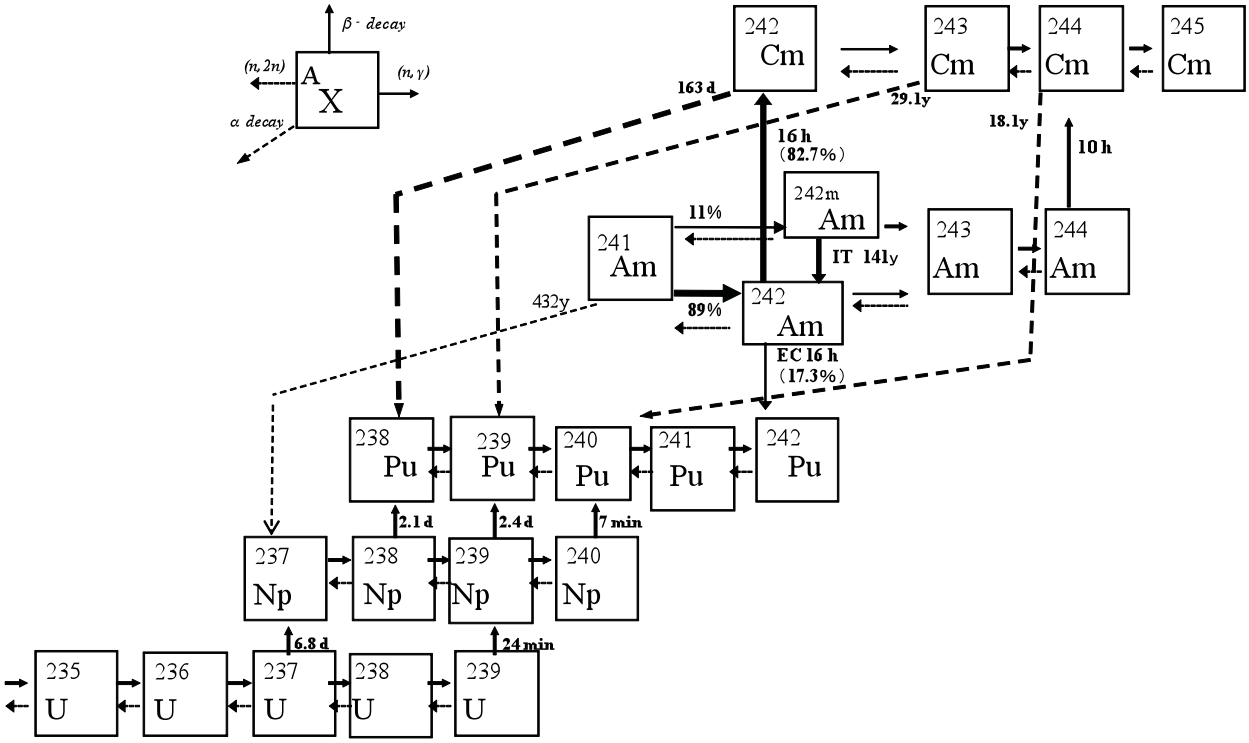

Figure 3. Nuclear Transmutation Chain considered in AFC-2A, 2B fuel analysis.

2.2 Methodology of Irradiation Analysis

Irradiation position EFT isolated model with boundary neutron source, SSR option in MCNP5 ver1.3, is applied. The depletion methodology MCWO (using ORIGEN2) was used to evaluate the AFC-2A, 2B fuel pin burnup behavior versus EFPD's within the ATR EFT positions.

The standard boundary neutron source was provided from the result of a full core as-run neutronics calculation. The model horizontal and vertical geometrical cross-sections are shown in Figure 4 and Figure 5. The fuel composition and specification are listed in Table 1. To calculate the neutron flux of each calculation cell, the ATR power history (Table 2) and following normalization factors were used to scale the MCNP-calculated flux tallies.

2.2.1 Neutron Flux Normalization Factor

Note, the MCNP f4 tally has units of 1/cm2 per source neutron.

$$Flux\ Normdization\ Coef\ f.[n/MW_{core}/\sec] = \left(\frac{Fis\ Neutrons}{Fis}\right)\left(\frac{Fis}{\text{MeV}}\right)\left(\frac{\text{MeV}}{MW_{core}\cdot\sec}\right)$$

$$= \left(\frac{2.43 Fis\ Neutrons}{Fis}\right)\left(\frac{Fis}{200\,\text{MeV}}\right)\left(\frac{6.2415\text{x}10^{18}\,\text{MeV}}{MW_{core}\cdot\sec}\right)$$

$$= 7.583\ \text{x}\ 10^{16}[Fis\ Neutrons/MW_{core}/\sec] \qquad \text{(Eq. 6)}$$

By using Eq.6, the neutron fluxes in AFC-2A and -2B position are calculated as Figure 6.

This isolated model is utilized to calculate the global uncertainty of each nuclide. The uncertainty information is applied to the depletion calculation results by full-core ATR model calculation. Though the isolated model has 5 to 10% discrepancy in the results of HM depletion and buildup from full core model, it still can provide good information in each differential coefficient in Eq.4 and in uncertainty ratio.

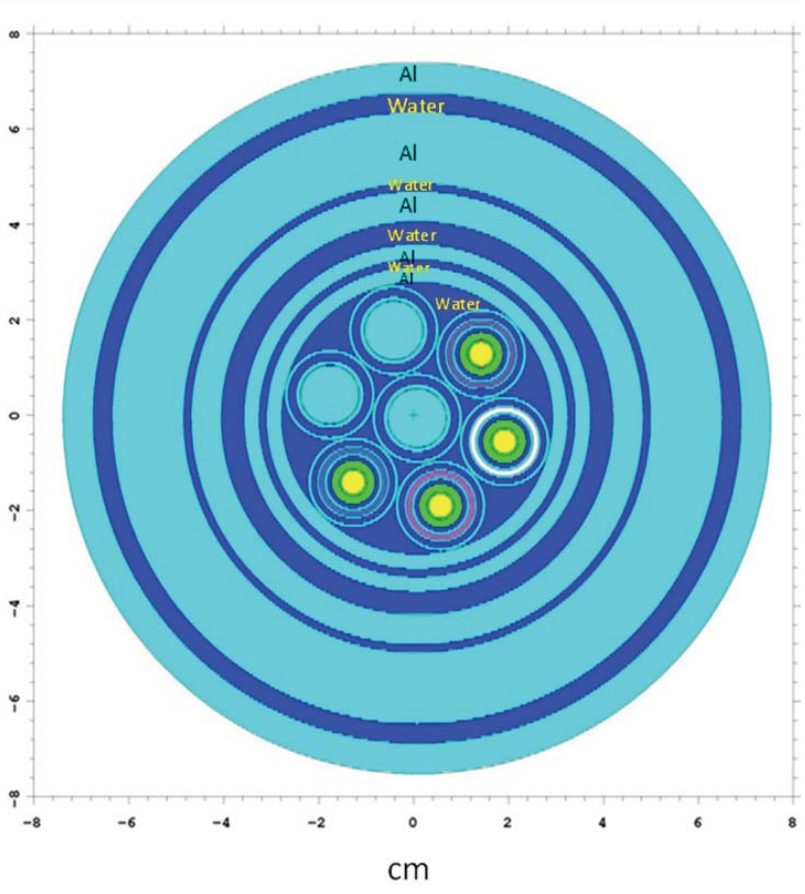

Figure 4. Horizontal cross-section of EFT with AFC-2A, 2B.

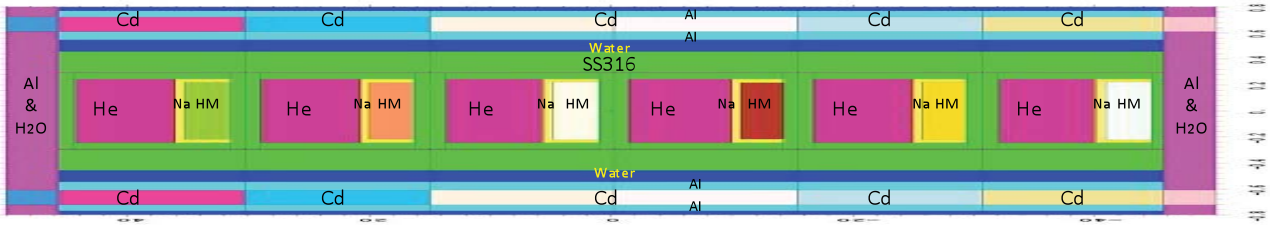

Figure 5 Vertical cross-section of E2 Capsule with AFC-2A rodlet

Table 1. AFC-2A & AFC-2B Fuel Test Matrix.

Rodlet	Metallic Fuel Alloy†	U-235 Enrichment
1	U-20Pu-3Am-2Np-15Zr	93%
2	U-20Pu-3Am-2Np-1.0RE*-15Zr	55%
3	U-20Pu-3Am-2Np-1.5RE*-15Zr	45%
4	U-30Pu-5Am-3Np-1.5RE*-20Zr	55%
5	U-30Pu-5Am-3Np-1.0RE*-20Zr	65%
6	U-30Pu-5Am-3Np-20Zr	93%

†Alloy composition expressed in weight percent.
*RE designates rare earth alloy (6% La, 16% Pr, 25% Ce, 53% Nd).

Table 2. Power history in Cycle 140A to 142B for MCWO calculation.

	ATR total Power [MWth]	Irradiation Time [days]	Cooling Time [days]
140A1	103.54	16	0
140A2	103.98	18	0
140A3	104.31	12.5	0
140A4	104.31	0	15
140B1	102.52	12	0
140B2	107.32	16	0
140B3	102.23	7.7	0
140B4	102.23	0	10
141A1	105.7	18	0
141A2	105.62	10	0
141A3	105.4	4.4	0
141A4	105.6	0	55
142A1	112.65	16	0
142A2	113.88	16	0
142A3	114.79	16	0
142A4	114.07	0	13
142B1	116.4	16	0
142B2	116.72	13.7	0
142B3	119.37	22.3	0
142B4	116.5	0	25

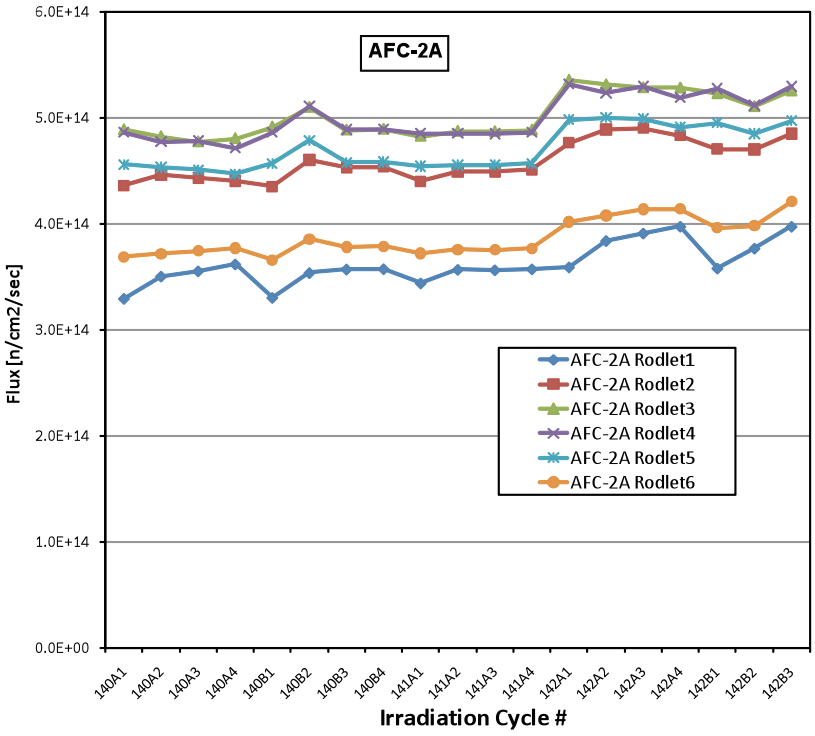

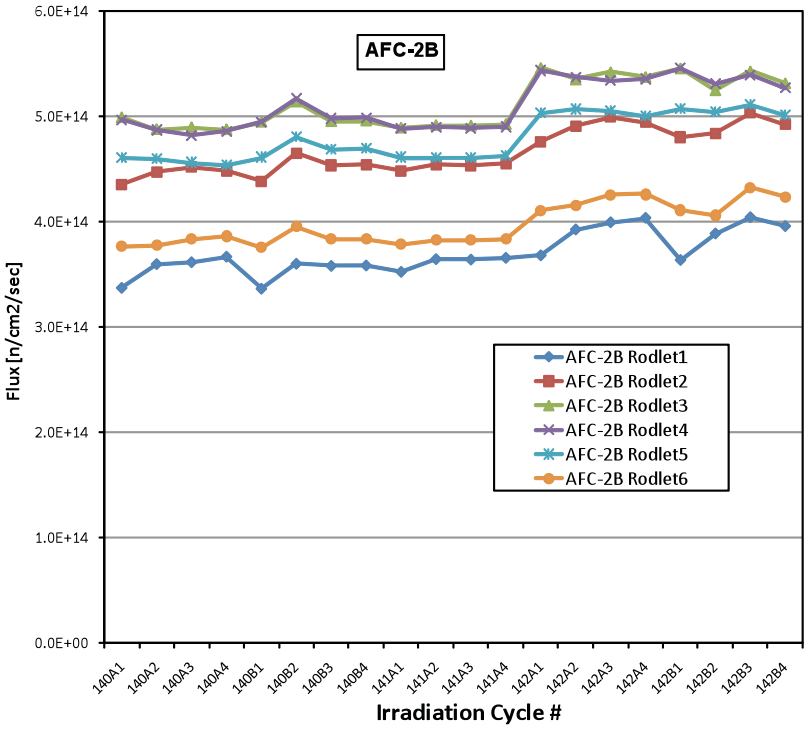

Figure 6. Neutron Flux in AFC-2A and AFC-2B fuel pin in each rodlet.

3. RESULTS AND DISCUSSION

The neutron cross-section error bands evaluated are: U-235, U-238, Np-237, and Pu-238 to Pu-242, Am-241, Am-243, and Cm-244. Nuclear reactions whose error data were not available are assumed as following; U-236 cross-section error is assumed to be the same as the U-238 data, Am-242m and Am-242 error is assumed the same as Am-241 data, and Cm-242, Cm-243 cross-section error are assumed to be the same as Cm-244 data. Due to the un-reliable (n,2n) cross-section, the (n,2n) cross-section error is assumed as 10%. The neutronics uncertainty analysis results and discussion are presented as follow.

3.1 Cross-Section Uncertainty

Cross-section uncertainty of each nuclide reaction type is calculated by ERRORJ code with 216 energy groups with constant lethargy width in relative value(%). Energy dependent reaction rate in AFC-2A, 2B position is also calculated. Since AFC-2A and -2B irradiation positions have a unique neutron spectrum due to Cd filter, there is no thermal neutron (<0.5eV) component, 50% of fast neutron (>0.1MeV) and 50% epi-thermal neutron (0.5eV<E<0.1MeV) as shown in Figure 7. For comparison, neutron spectrum of typical fast reactors and PWR are also drawn in the figure. As shown in the figure, AFC-2A and -2B position neutron spectrum contains more epithermal neutron than typical fast reactor, epi-thermal neutrons are very important for the capture reaction and fissile nuclide fission reactions.

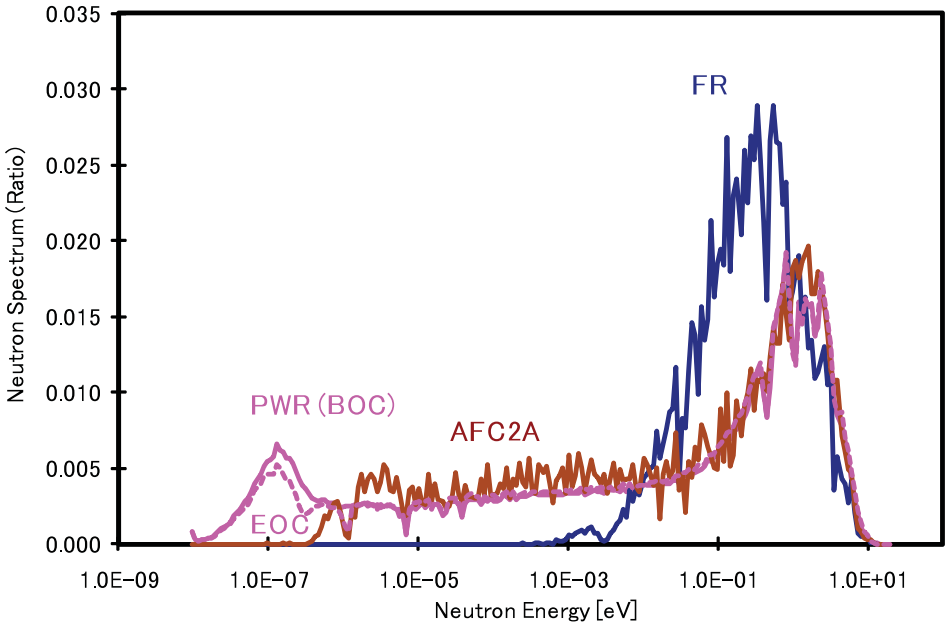

Figure 7. Neutron Spectrum in AFC-2A. (AFC2A: AFC-2A rodlet 3 fuel pin averaged spectrum FR: Fast Rector inner core averaged spectrum with MOX(U0.7,Pu0.3) with Na as coolant PWR: PWR pin averaged spectrum with 3.5% enriched UOX)

Cross-section uncertainty of each nuclide, reaction type (capture, fission and n,2n if nuclear data available) is shown in Figure 9 to Figure 18. Energy dependent reaction rate is also shown in the same figures to evaluate the importance of energy to the cross-section error. Because of the similarity of the neutron spectrum in AFC-2A and AFC-2B fuel pins, only AFC-2A position spectrum is used for the analysis as being representative of AFC-2A and AFC-2B spectrum.

Uranium-235 cross-section errors are shown in Figure 9. The covariance data of U-235 is derived from JENDL3.3. Since there is abundant measurement data for U-235, the effective one-group capture cross-section error in AFC-2A is calculated as 1%. In neutron fission reaction, the effective one-group capture cross-section error in AFC-2A is calculated as 1%. In n, 2n reaction, the effective one-group (n,2n) cross-section error in AFC-2A is calculated as 10%.

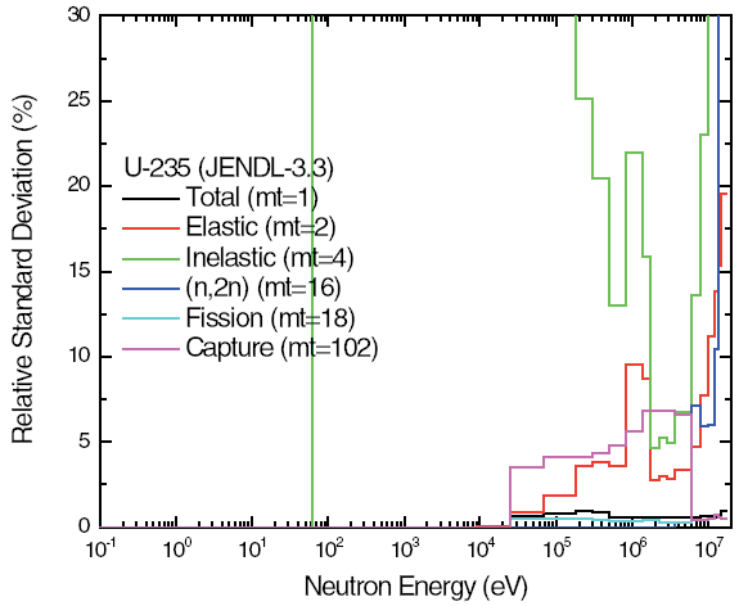

Figure 8. U-235 Energy Dependent Cross-Section Error.[17]

Uranium-238 cross-section error and reaction rate in AFC-2A are shown in Figure 9. Neutron capture cross-section error and reaction rate are shown in Figure 9(a), fission cross-section error and reaction rate are shown in Figure 9(b), n,2n cross-section error and reaction rate are shown in Figure 9(c). The covariance data of U-238 is derived from JENDL3.3. In neutron capture reaction, due to the unique neutron spectrum in AFC 2A, all the neutron capture reactions occurred with epi-thermal neutrons in resonance capture. Since there is abundant measurement data for U-238, capture cross-section error in epi-thermal energy range is as low as about 3%, and the effective one-group capture cross-section error in AFC-2A is calculated as 3%. In neutron fission reaction, due to the threshold fission cross-section of U-238 at about 1MeV, all the neutron fission reactions occurred with fast neutrons, the effective one-group capture cross-section error in AFC-2A is calculated as 1%. In n,,2n reaction, the effective one-group (n,2n) cross-section error in AFC-2A is calculated as 3%.

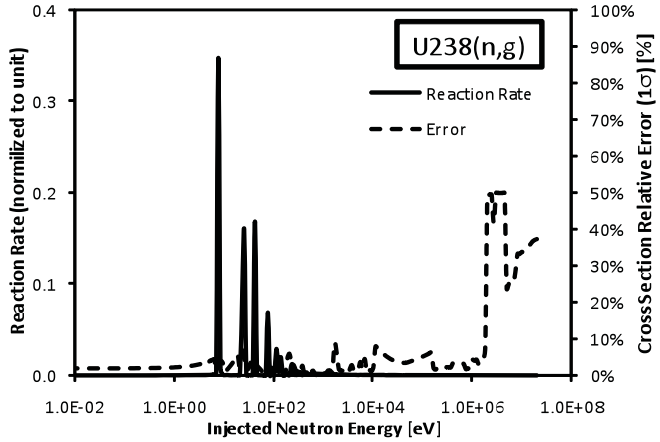

(a) Capture Reaction Rate and Cross Section Error

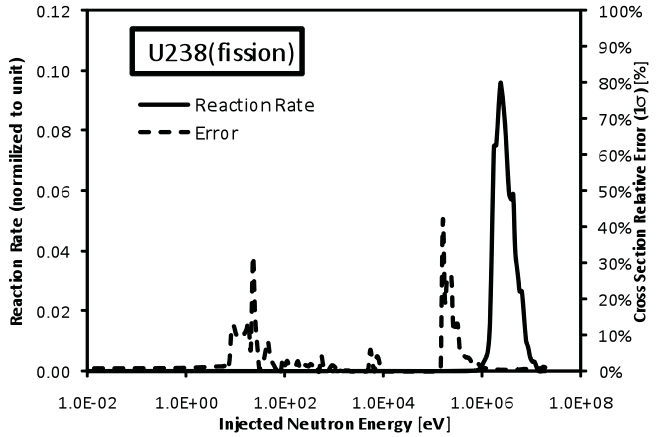

(b) Fission Reaction Rate and Cross Section Error

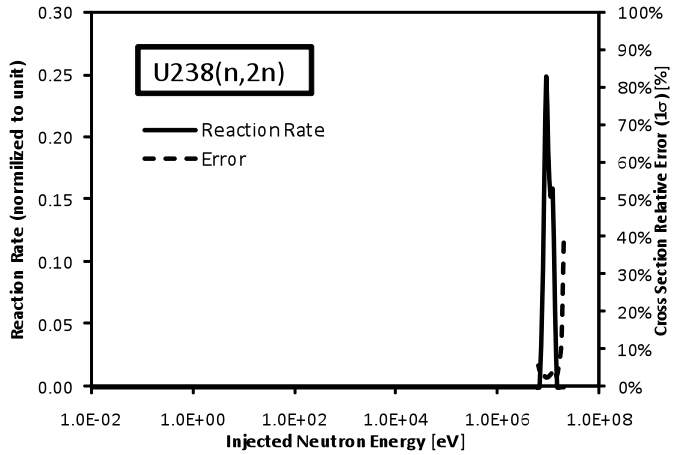

(c) (n,2n) Reaction Rate and Cross Section Error

Figure 9. U-238 Energy Dependent Reaction Rate in AFC 2A and Cross-Section Error.

Neptunium-237 cross-section error and reaction rate in AFC-2A are shown in Figure 10. Neutron capture cross-section error and reaction rate are shown in Figure 10(a), fission cross-section error and reaction rate are shown in Figure 10(b). The covariance data of Np-237 is derived from both JENDL3.3 and Low-fidelity Covariance. The figures and tables in the present report illustrate evaluations with JENDL3.3 as representative. In neutron capture reaction, due to the unique neutron spectrum in AFC 2A, almost all the neutron capture reactions are resonance capture with epi-thermal neutrons around 0.6eV and 1.7eV. The effective one-group capture cross-section error in AFC-2A is calculated as 5%. The neutron fission reaction, due to large fast fission cross-section of Np-237 in hundreds KeV and resonance fission in tens to hundreds eV, occur with mostly fast neutrons and partly epithermal neutrons, the effective one-group fission cross-section error in AFC-2A is calculated as 3%.

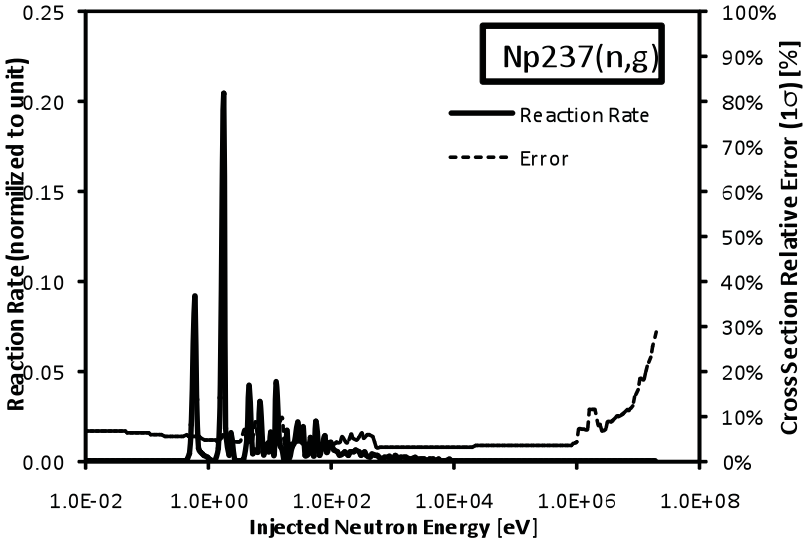

(a) Capture Reaction Rate and Cross Section Error

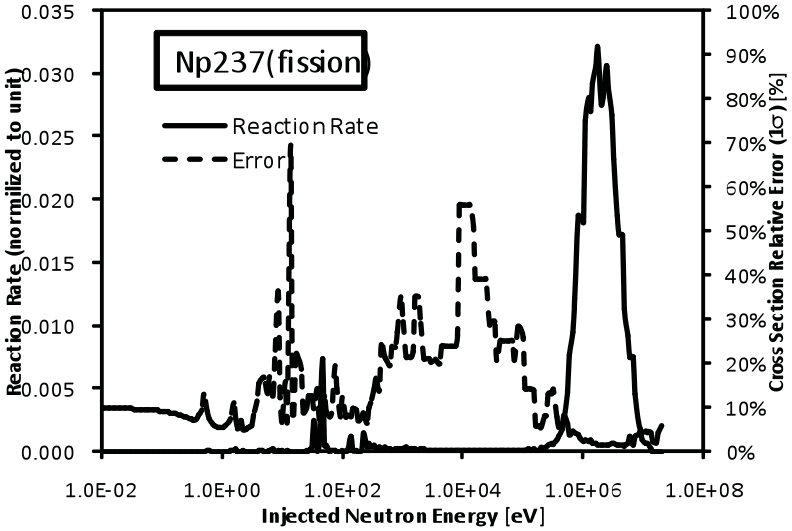

(b) Fission Reaction Rate and Cross Section Error

Figure 10. Np-237 Energy Dependent Reaction Rate in AFC 2A and Cross-Section Error.

Plutonium-238 cross-section error and reaction rate in AFC-2A are shown in Figure 11. Neutron capture cross-section error and reaction rate are shown in Figure 11(a), fission cross-section error and reaction rate are shown in Figure 11(b). The covariance data of Pu-238 is derived from both JENDL3.3 and Low-fidelity Covariance The figures and tables in the present report illustrate JENDL3.3 data as representative. In neutron capture reaction, due to the unique neutron spectrum in AFC 2A, almost all the neutron capture reactions are occurred with epi-thermal neutron in resonance capture. Due to the large uncertainty in broader energy range, the effective one-group capture cross-section error in AFC-2A is calculated as 27%. In neutron fission reaction, due to fast fission and large resonance fission in one to hundreds eV, neutron fission reactions are occurred broadly with from epithermal to fast neutron, the effective one-group fission cross-section error in AFC-2A is calculated as 18%.

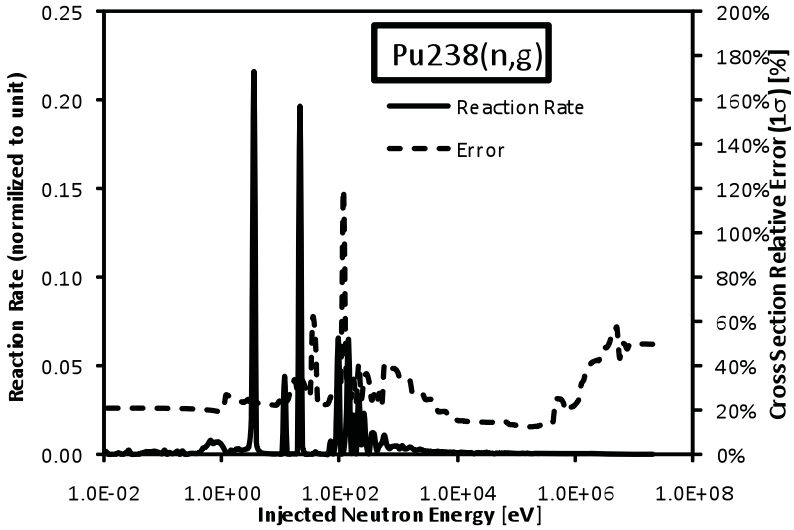

(a) Capture Reaction Rate and Cross Section Error

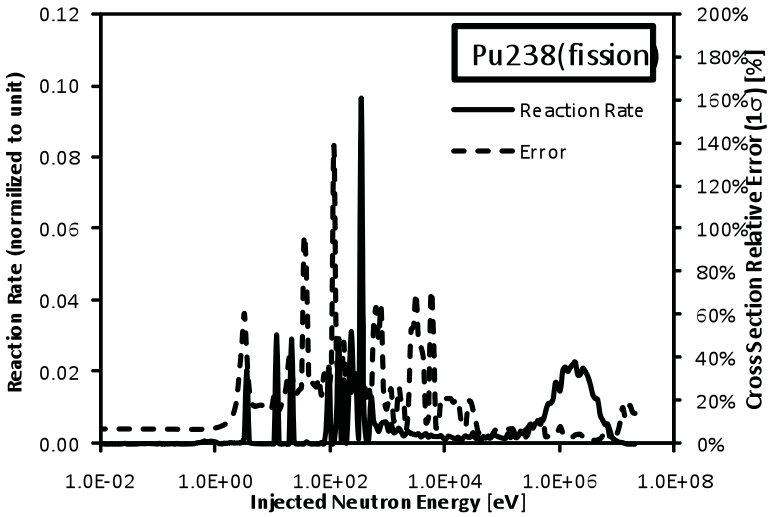

(b) Fission Reaction Rate and Cross Section Error

Figure 11. Pu-238 Energy Dependent Reaction Rate in AFC 2A and Cross-Section Error.

Plutonium-239 cross-section error and reaction rate in AFC-2A are shown in Figure 12. Neutron capture cross-section error and reaction rate are shown in Figure 12(a), fission cross-section error and reaction rate are shown in Figure 12(b), n,2n cross-section error and reaction rate are shown in Figure 12(c). The covariance data of Pu-239 is derived from JENDL3.3. For neutron capture reaction, due to the unique neutron spectrum in AFC 2A, almost all the neutron capture reactions occurred with epi-thermal neutrons in resonance capture. The effective one-group capture cross-section error in AFC-2A is calculated as 4%. Neutron fission reactions, due to fast fission and large resonance fission, occur broadly from epithermal to fast neutron energy. The effective one-group fission cross-section error in AFC-2A is calculated as 6%. In n,2n reaction, due to the large error in nuclear data, the effective one-group (n,2n) cross-section error in AFC-2A is calculated as 205%. However, the one-group (n,2n) cross-section is very small in ATR test position. Its impact on the calculated MA inventories is negligible.

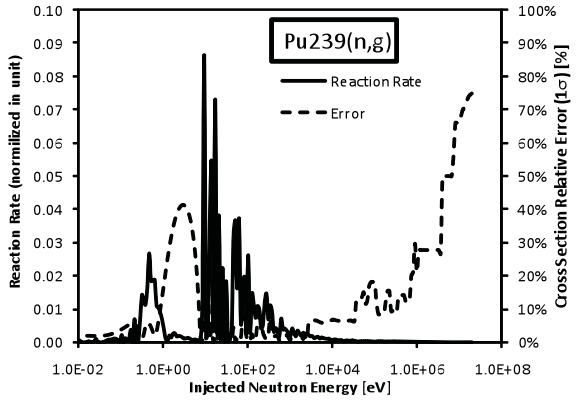

(a) Capture Reaction Rate and Cross Section Error

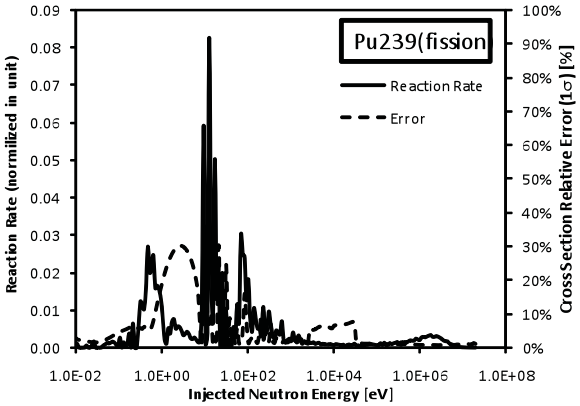

(b) Fission Reaction Rate and Cross Section Error

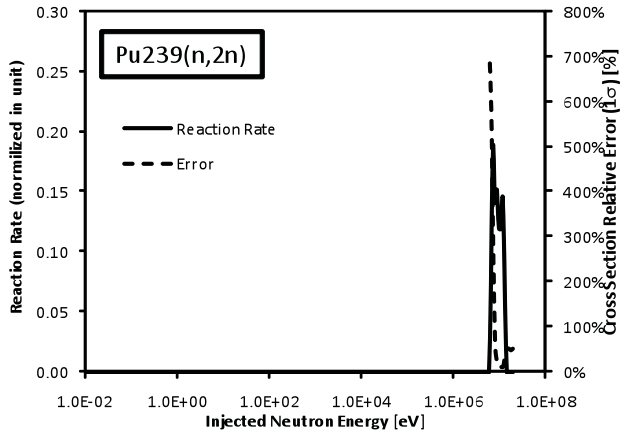

(c) (n,2n) Reaction Rate and Cross Section Error

Figure 12. Pu-239 Energy Dependent Reaction Rate in AFC 2A and Cross-Section Error.

Plutonium-240 cross-section error and reaction rate in AFC-2A are shown in Figure 13. Neutron capture cross-section error and reaction rate are shown in Figure 13(a), fission cross-section error and reaction rate are shown in Figure 13(b), n,2n cross-section error and reaction rate are shown in Figure 13(c). The covariance data of Pu-240 is derived from both JENDL3.3 and Low-Fidelity Covariance, while figures and tables in the present report show evaluations with JENDL3.3 as representative. In neutron capture reaction, due to the unique neutron spectrum in AFC 2A, almost all the neutron capture reactions occurred with epi-thermal neutrons in about 1 eV resonance capture. The effective one-group capture cross-section error in AFC-2A is calculated as 2%. In the neutron fission reaction, due to large fast fission and partly resonance fission, reactions occurred with mostly fast neutrons and partly epi-thermal neutrons. The effective one-group fission cross-section error in AFC-2A is calculated as 1%. In n,2n reaction, due to the large error in nuclear data, the effective one-group (n,2n) cross-section error in AFC-2A is calculated as 25%.

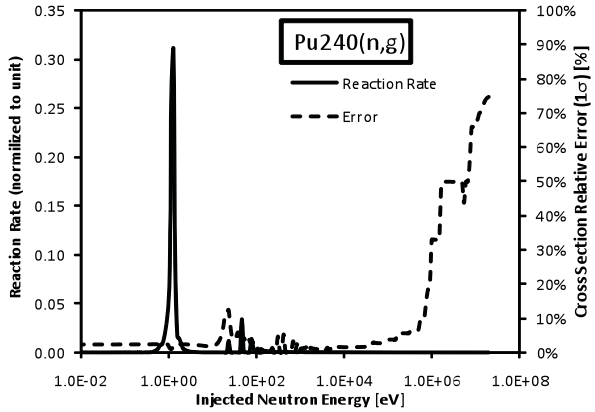

(a) Capture Reaction Rate and Cross Section Error

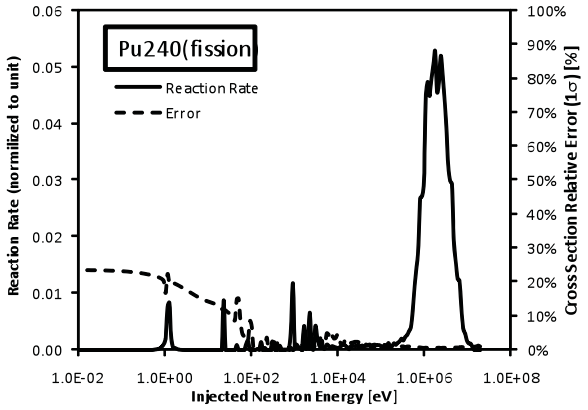

(b) Fission Reaction Rate and Cross Section Error

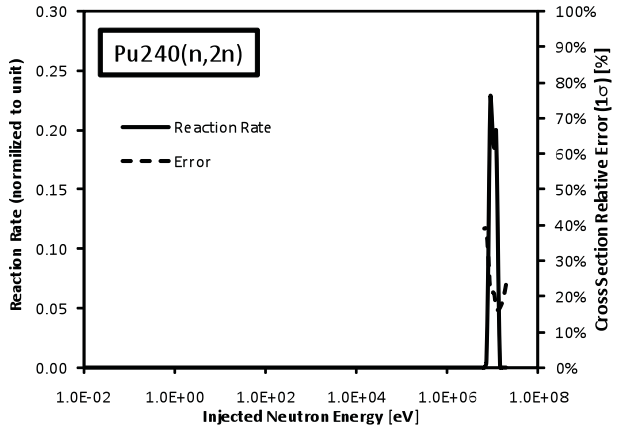

(c) (n,2n) Reaction Rate and Cross Section Error

Figure 13. Pu-240 Energy Dependent Reaction Rate in AFC 2A and Cross-Section Error.

Plutonium-241 cross-section error and reaction rate in AFC-2A are shown in Figure 14. Neutron capture cross-section error and reaction rate are shown in Figure 14(a), fission cross-section error and reaction rate are shown in Figure 14(b), n,2n cross-section error and reaction rate are shown in Figure 14(c). The covariance data of Pu-241 is derived from both JENDL3.3 and Low-Fidelity Covariance, and figures and tables in the present report present evaluations with JENDL3.3 as representative. In neutron capture reaction, due to the unique neutron spectrum in AFC 2A, almost all the neutron capture reactions occurred with epi-thermal neutrons in resonance capture. The effective one-group capture cross-section error in AFC-2A is calculated as 0.5%. Neutron fission reaction, due to fast fission and large resonance fission, occurred broadly with epithermal to fast neutrons. The effective one-group fission cross-section error in AFC-2A is calculated as 0.3%. In n,2n reaction, due to the large error in nuclear data, the effective one-group (n,2n) cross-section error in AFC-2A is calculated as 5%.

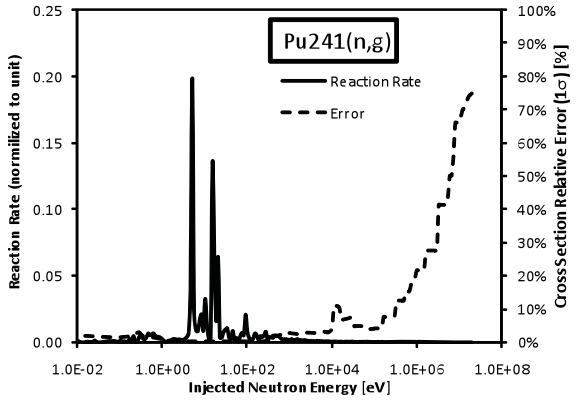

(a) Capture Reaction Rate and Cross Section Error

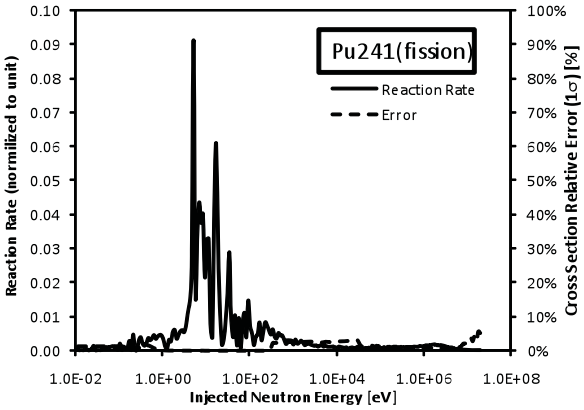

(b) Fission Reaction Rate and Cross Section Error

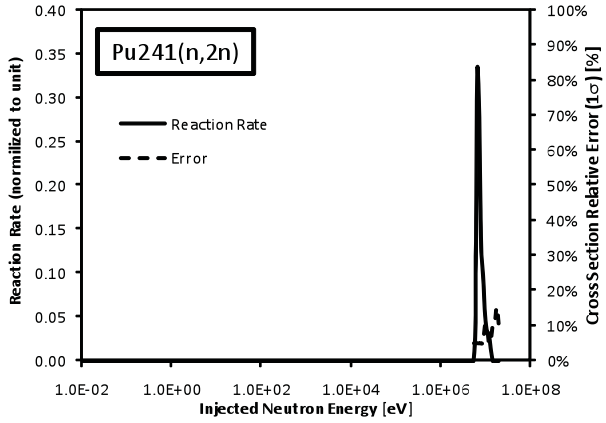

(c) (n,2n) Reaction Rate and Cross Section Error

Figure 14. Pu-241 Energy Dependent Reaction Rate in AFC 2A and Cross-Section Error.

Plutonium-242 cross-section error and reaction rate in AFC-2A are shown in Figure 15. Neutron capture cross-section error and reaction rate are shown in Figure 15(a), fission cross-section error and reaction rate are shown in Figure 15(b). The covariance data of Pu-240 is derived from both JENDL3.3 and Low-Fidelity Covariance, and figures and tables in the present report show evaluations with JENDL3.3 as representative. In neutron capture reaction, due to the unique neutron spectrum in AFC 2A, almost all the neutron capture reactions occurred with epi-thermal neutron, 3eV, resonance capture. The effective one-group capture cross-section error in AFC-2A is calculated as 4%. Neutron fission reaction, due to large fast fission and partial resonance fission, occurred with mostly fast neutron and partially epi-thermal neutrons, the effective one-group fission cross-section error in AFC-2A is calculated as 4%.

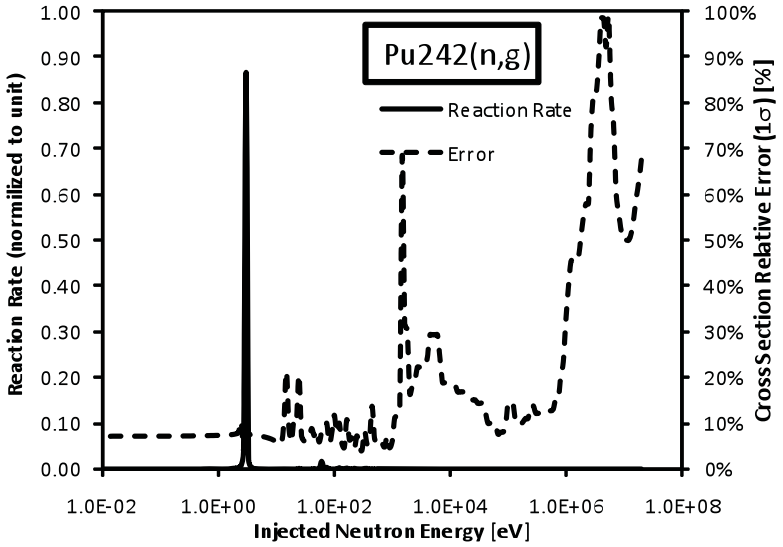

(a) Capture Reaction Rate and Cross Section Error

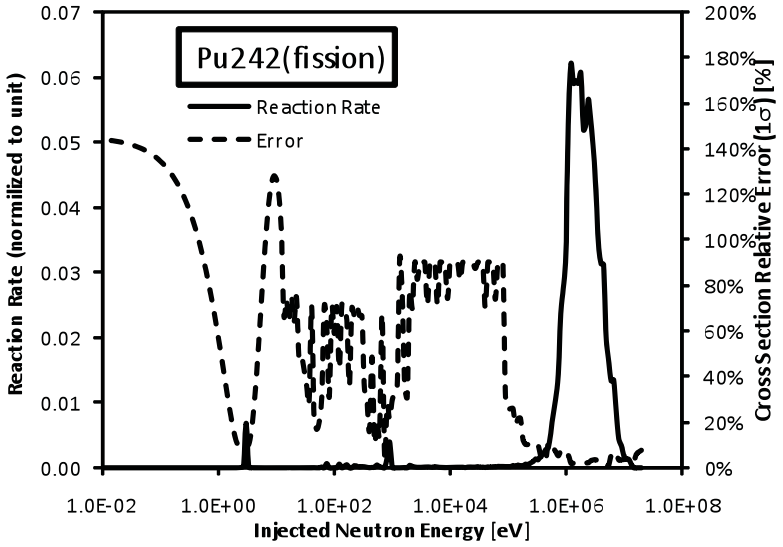

(b) Fission Reaction Rate and Cross Section Error

Figure 15. Pu-242 Energy Dependent Reaction Rate in AFC 2A and Cross-Section Error.

Americium-241 cross-section error and reaction rate in AFC-2A are shown in Figure 16. Neutron capture cross-section error and reaction rate are shown in Figure 16(a), fission cross-section error and reaction rate are shown in Figure 16(b). The covariance data of Am-241 is derived from both JENDL3.3 and Low-Fidelity Covariance, with figures and tables in the present report evaluated with JENDL3.3 as representative. In neutron capture reaction, due to the unique neutron spectrum in AFC 2A, almost all the neutron capture reactions occurred with epi-thermal neutrons. The effective one-group capture cross-section error in AFC-2A is calculated as 12%. Neutron fission reaction, due to large fast fission and partial resonance fission, occurred with mostly fast neutron and partly epi-thermal neutrons. The effective one-group fission cross-section error in AFC-2A is calculated as 6%.

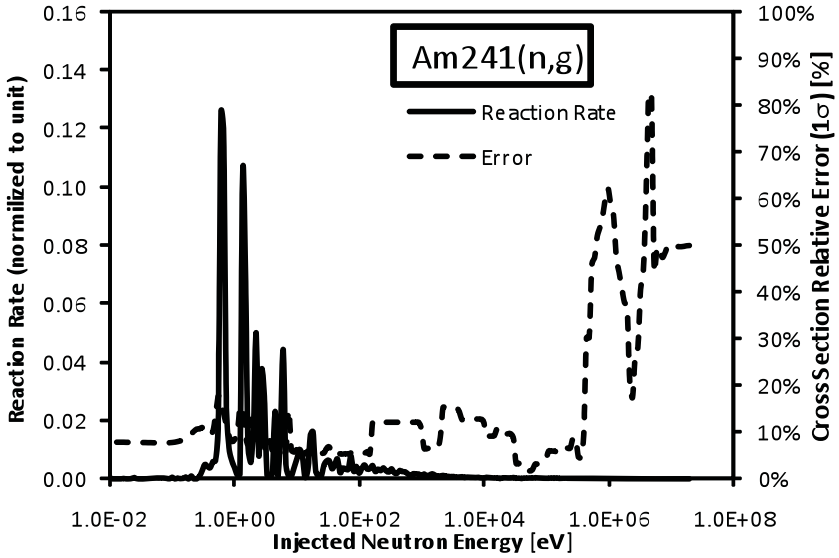

(a) Capture Reaction Rate and Cross Section Error

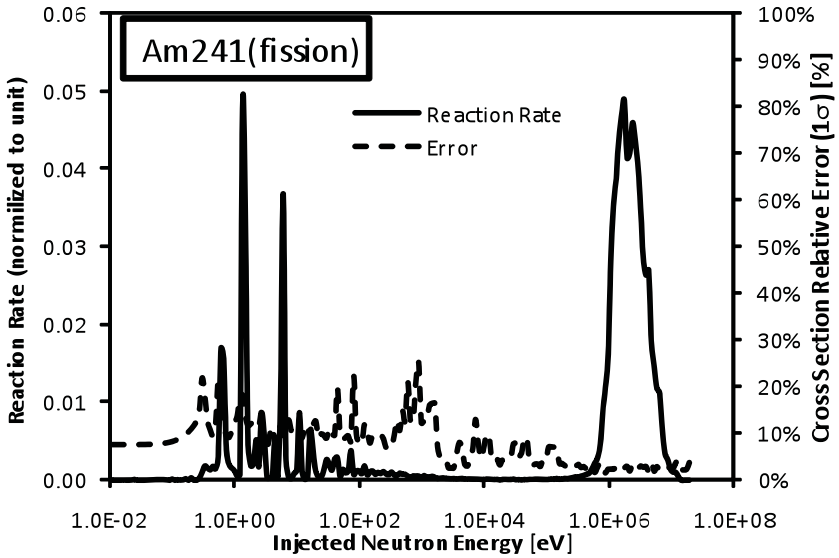

(b) Fission Reaction Rate and Cross Section Error

Figure 16. Am-241 Energy Dependent Reaction Rate in AFC 2A and Cross-Section Error.

Americium-243 cross-section error and reaction rate in AFC-2A are shown in Figure 17. Neutron capture cross-section error and reaction rate are shown in Figure 17(a), fission cross-section error and reaction rate are shown in Figure 17(b). The covariance data of Pu-243 is derived from both JENDL3.3 and Low-Fidelity Covariance, and figures and tables in the present report present JENDL3.3 results as representative. In neutron capture reaction, due to the unique neutron spectrum in AFC 2A, almost all the neutron capture reactions occurred with epi-thermal neutron from one to tens of eV. The effective one-group capture cross-section error in AFC-2A is calculated as 7%. In neutron fission reaction, due to large fast fission and partial resonance fission, neutron fission reactions occurred with mostly fast neutron and partly epi-thermal neutrons, the effective one-group fission cross-section error in AFC-2A is calculated as 6%.

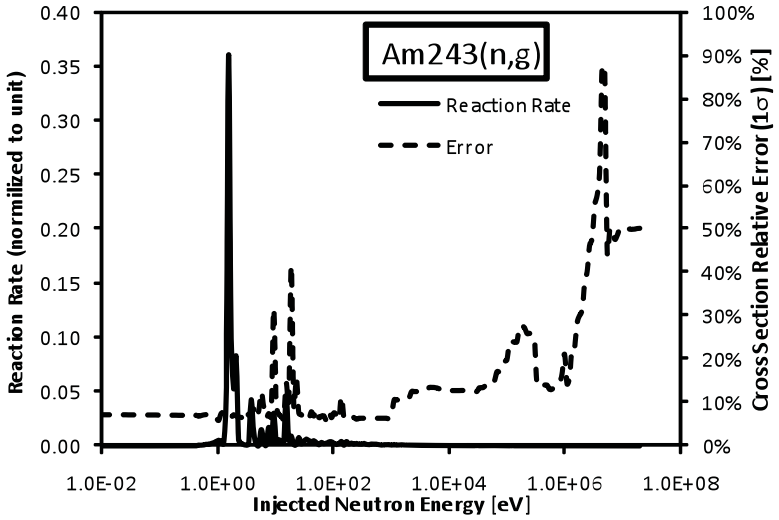

(a) Capture Reaction Rate and Cross Section Error

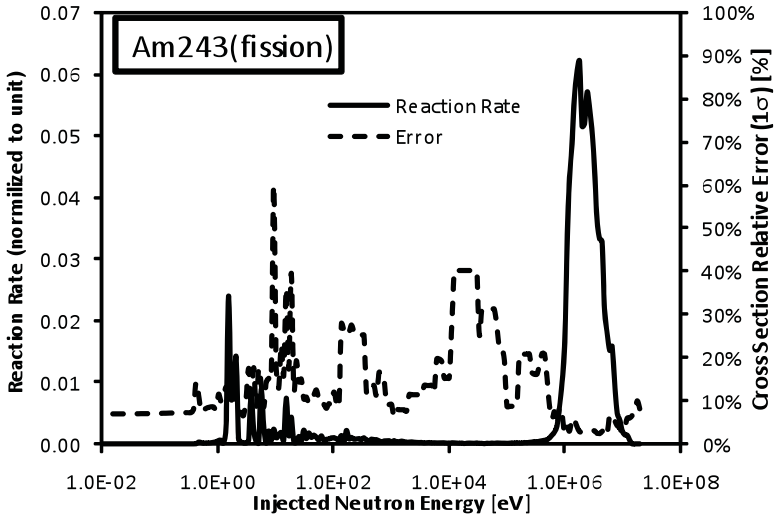

(b) Fission Reaction Rate and Cross Section Error

Figure 17. Am-243 Energy Dependent Reaction Rate in AFC 2A and Cross-Section Error.

Curium-244 cross-section error and reaction rate in AFC-2A are shown in Figure 18. Neutron capture cross-section error and reaction rate are shown in Figure 18(a), fission cross-section error and reaction rate are shown in Figure 18(b). The covariance data of Cm-244 is derived from both JENDL3.3 and Low-Fidelity Covariance, and figures and tables in the present report were evaluated with JENDL3.3 and are shown as representative. Neutron capture reaction, due to the unique neutron spectrum in AFC 2A, almost all occurred with epi-thermal neutrons from one to tens of eV. Due to large cross-section error, the effective one-group capture cross-section error in AFC-2A is calculated as 22%. Neutron fission reaction, due to large fast fission and partial resonance fission, neutron fission reactions occurred with mostly fast neutron and partly epi-thermal neutrons. The effective one-group fission cross-section error in AFC-2A is calculated as 19%.

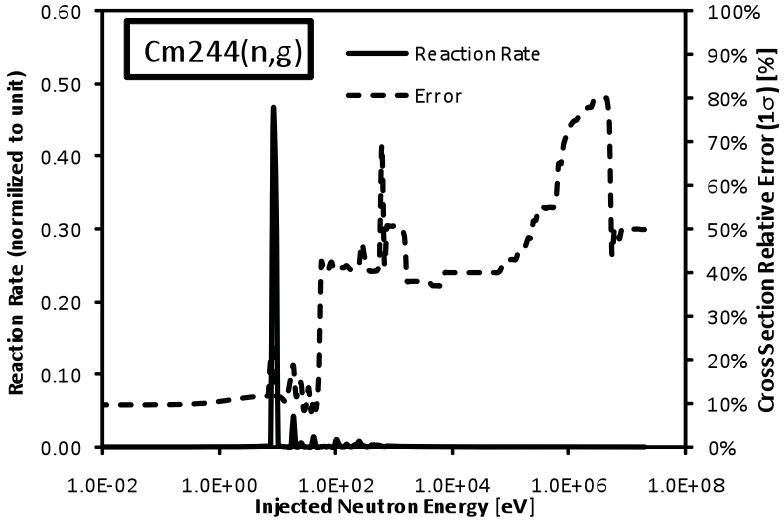

(a) Capture Reaction Rate and Cross Section Error

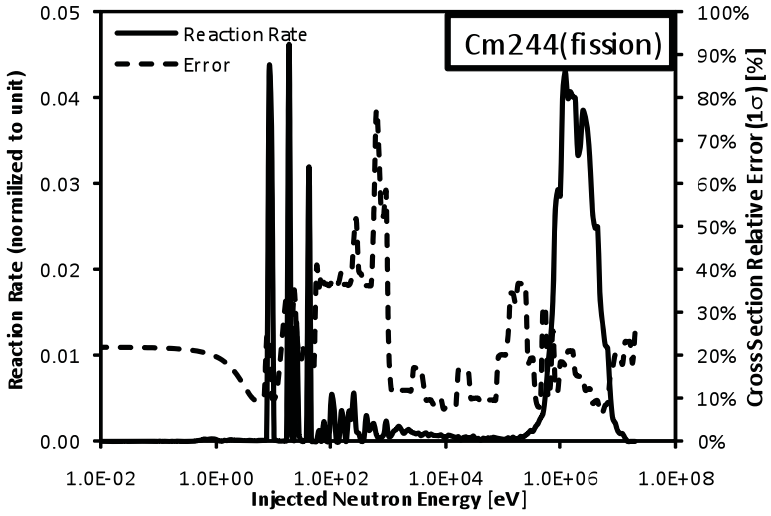

(b) Fission Reaction Rate and Cross Section Error

Figure 18. Cm-244 Energy Dependent Reactions Rate in AFC 2A and Cross-Section Error.

As a summary of the evaluation of effective cross-section error in AFC-2A, all cross-section errors of all nuclides and reactions are summarized in Table 3.

Table 3. Effective Cross-Section Relative Uncertainty (1-σ) in AFC-2A position.

	Nuclear Reactions		
	fission	capture	n.2n
U235	1%	1%	10%
U238	1%	3%	3%
NP237	3%	5%	
PU238	18%	27%	
PU239	6%	4%	205%
PU240	1%	2%	25%
PU241	0.3%	0.5%	5%
PU242	4%	4%	
AM241	6%	12%	
AM243	5%	7%	
CM244	19%	22%	

3.2 Depletion and Buildup Calculation Results and Global Uncertainty

By using Table 3, global uncertainty analysis of HM depletion and buildup has been performed. As- run depletion and buildup calculations are performed using the MCWO code, and by applying the error data in Table 3. Additional depletion and buildup calculations are also performed to calculate the global uncertainty of each nuclide by using Eq. 5.

3.2.1 HM Isotope Density

Table 4 shows the atomic density of HM in AFC-2A and -2B at the end of irradiation cycle 142B. Table 4(a) is the atomic density of uranium and neptunium isotopes, Table 4(b) is the atomic density of plutonium isotopes, Table 4(c) is the atomic density of americium isotopes, and Table 4(d) is the atomic density of curium isotopes. As for the reference, initial HM load at the beginning of irradiation of cycle 140A is listed in Table 5.

In Table 4(a), since initial uranium enrichment and loading are different in each position and each rodlet as shown in Table 1, the atomic density of uranium isotopes at the end of Cycle 142B is varied. Uranium-235 has the same cross-section errors for capture and fission reactions (1%), and due to massive initial load, the uncertainty of U-235 atomic density at the end of irradiation is quite small, 0.1%. On the other hand, U-236 has no initial load and it is accumulated from the U-235(n,g) reaction, the uncertainty of U-236 is mainly affected by that reaction and is around 1%. The sensitivity of cross-section errors to U-236 atom density uncertainty is shown in Figure 19. Both U-235(n,g) and U-235(n,f) cross-section error are affecting the U-236 atom density uncertainty and the majority is, as expected, U-235(n,g) cross-section error. Sensitivity of U-236 cross-section error is negligibly small because of the massive initial load of U-235. Uranium-238 has massive initial load and small cross-section error (1% U-238(n,f) and 3% U-238(n,g)), so the uncertainty of U-238 atom density after the irradiation is very low, 0.05%.

Neptunium-237 has rather large resonance capture cross-section at 0.6eV and 1.7eV, depletion ratio is varied from 10-17% in AFC-2A and -2B rodlets, and its effective cross-section error is 5% in capture and

3% in fission. However, due to the initial load of Np-237, the uncertainty of atomic density is kept less than 1% (Table 4(a)). The sensitivity of cross-section errors to Np-237 atom density uncertainty is shown in Figure 20. Uranium-235(n,g), U-236(n,g), Np-237(n,g) and Np-237(n,f) cross-section errors are affecting the Np-237 atom density uncertainty and the majority is by Np-237(n,g) cross-section error.

Table 4(b) shows the atomic density of plutonium isotopes. Though major isotopes such as Pu-239, Pu-240 and Pu-241 have small uncertainty of atomic density, the minor isotopes, Pu-238 and Pu-242 have relatively large uncertainty of atomic density. The sensitivity of cross-section errors to Pu-238 atom density uncertainty is shown in Figure 21. Various factors are affecting the uncertainty of Pu-238 because it is the daughter nuclide of Np-237 and Am-241 transmutation, and especially Am-241(n,g), Np-237(n,g) and Pu-238(n,g) errors are the major factors to the uncertainty. The sensitivity of cross-sections errors to Pu-242 atom density uncertainty is shown in Figure 22. Americium-241(n,g), Pu-242(n,g) and Pu-240(n,g) are affecting the uncertainty of Pu-242. As shown in the transmutation chain(Figure 3), there are mainly 2 paths to build up Pu-242, one is the Pu-241(n,g)->Pu-242 and the other is Am-241(n,g)-> Am-242(EC) -> Pu-242. Since the Am-241(n,g) cross section and its error are relatively large, Am-241(n,g) errors work as major factors to the uncertainty.

Table 4(c) is the atomic density of americium isotopes. Initial load of Am consisted of pure Am-241. It has a large capture cross section and depletion ratio were observed from 17 to 27% in AFC-2A, 2B rodlets, and the cross section error of the nuclide is also large(6% in fission and 12% in capture reaction). Transmutation of Am-241 affect very much the daughter accumulation and their uncertainty, Am-242m and Am-243 have 13% uncertainty of their atom density. The sensitivity of cross-sections errors to Am-241 atom density uncertainty is shown in Figure 23. Americium-241(n,g) and Am-241(n,f) are affecting the uncertainty of Am-241, and Am-241(n,g) error is the dominant factor of the uncertainty. The sensitivity of cross-sections errors to Am-243 atom density uncertainty is shown in Figure 24Figure 19. As shown in the transmutation chain(Figure 3), there are mainly 2 paths to build up Am-243. One is the Pu-242(n,g)->Am-243 and the other is Am-241(n,g)-> Am-242m -> Am-243, and Am-241(n,g), Pu-242(n,g) errors are the major factors to the uncertainty.

Table 4(d) is the atomic density of curium isotopes. There is no initial load of Cm, so all Cm is accumulated through the transmutation of Am. Cm-244 has shortage of measurement and large cross section errors (19% in fission and 22% in capture). Since the same error as Cm-244 is applied to other Cm isotopes in the present work, the uncertainty of Cm isotopes is very large. The sensitivity of cross-sections errors to Cm-242 atom density uncertainty is shown in Figure 25. Americium-241(n,g) and Cm-242(n,g) are affecting the uncertainty of Cm-242 atom density, and Am-241(n,g) error is the dominant factor of the uncertainty. The sensitivity of cross-sections errors to Cm-244 atom density uncertainty is shown in Figure 26. As shown in the transmutation chain(Figure 3), there are mainly 2 paths to build up Cm-244. One is the Am-243(n,g)->Cm-244 and the other is Cm-243(n,g)-> Cm-244, and Pu-242(n,g) and Am-241(n,g) errors are the major factors to the uncertainty.

Time dependent HM depletion with uncertainty is shown in Figure 27, for AFC-2A rodlet 3. Nuclides relating with MA transmutation are selected in the figure to confirm the transport of errors by nuclides and by irradiation time.

Table 4(a). Atomic Density of U, Np (Cycle 142B EOC).

		U235 [#/b/cm]	Δ [%]	U236 [#/b/cm]	Δ [%]	U238 [#/b/cm]	Δ [%]	Np237 [#/b/cm]	Δ [%]
AFC-2A	Rodlet1	1.971E-02	0.1%	5.47E-04	1%	1.328E-03	0.05%	7.05E-04	0.9%
	Rodlet2	1.278E-02	0.1%	4.76E-04	1%	7.100E-03	0.05%	6.81E-04	0.9%
	Rodlet3	8.371E-03	0.1%	3.78E-04	1%	1.098E-02	0.05%	6.19E-04	0.9%
	Rodlet4	7.672E-03	0.1%	3.29E-04	1%	6.456E-03	0.05%	1.22E-03	0.9%
	Rodlet5	8.196E-03	0.1%	3.33E-04	1%	4.511E-03	0.05%	9.49E-04	0.9%
	Rodlet6	1.183E-02	0.1%	3.77E-04	1%	7.449E-04	0.05%	9.94E-04	0.9%
AFC-2B	Rodlet1	1.945E-02	0.1%	5.46E-04	1%	1.313E-03	0.05%	6.46E-04	0.9%
	Rodlet2	1.271E-02	0.1%	4.80E-04	1%	7.076E-03	0.05%	6.20E-04	0.9%
	Rodlet3	8.383E-03	0.1%	3.73E-04	1%	1.100E-02	0.05%	5.90E-04	0.9%
	Rodlet4	7.901E-03	0.1%	3.48E-04	1%	6.661E-03	0.05%	8.70E-04	0.9%
	Rodlet5	8.034E-03	0.1%	3.90E-04	1%	4.438E-03	0.05%	8.46E-04	0.9%
	Rodlet6	1.186E-02	0.1%	3.93E-04	1%	7.467E-04	0.05%	8.73E-04	0.9%

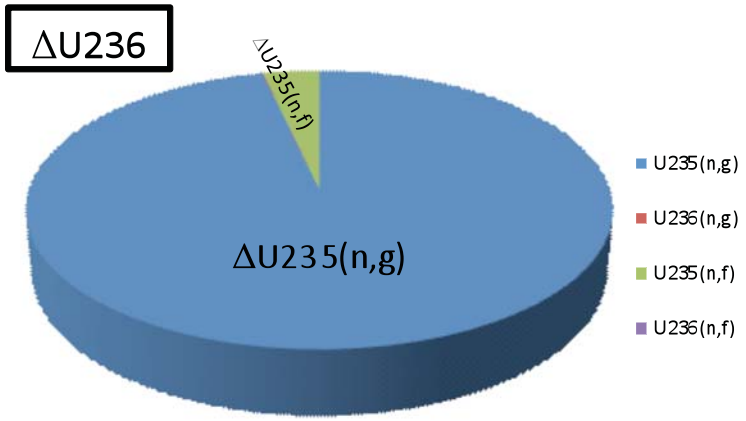

Figure 19. Sensitivity of cross section error to ΔU236, Density Uncertainty.

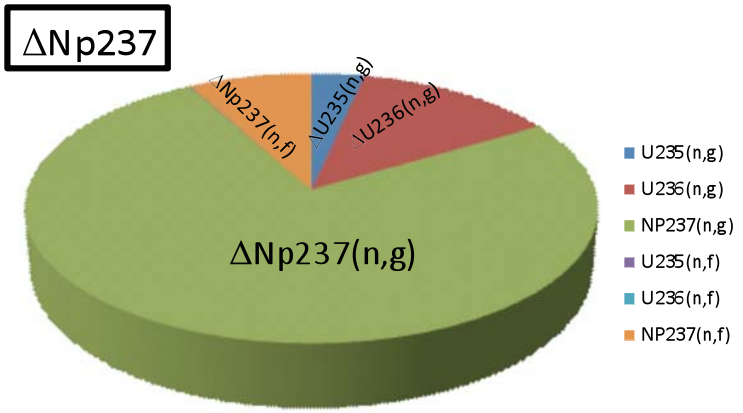

Figure 20. Sensitivity of cross section error to ΔNp237, Density Uncertainty.

Table 4(b). Atomic Density of Pu (Cycle 142B EOC).

		Pu238 [#/b/cm]	Δ [%]	Pu239 [#/b/cm]	Δ [%]	Pu240 [#/b/cm]	Δ [%]	Pu241 D[#/b/cm]	Δ [%]	Pu242 [#/b/cm]	Δ [%]
AFC-2A	Rodlet1	1.54E-04	7%	5.578E-03	0.6%	1.11E-03	1%	2.35E-04	2%	5.43E-05	10%
	Rodlet2	2.03E-04	7%	5.331E-03	0.6%	9.39E-04	1%	2.90E-04	2%	5.93E-05	10%
	Rodlet3	2.21E-04	7%	5.300E-03	0.6%	1.04E-03	1%	3.32E-04	2%	6.84E-05	10%
	Rodlet4	3.29E-04	7%	8.148E-03	0.6%	1.53E-03	1%	3.96E-04	2%	8.58E-05	10%
	Rodlet5	2.81E-04	7%	7.449E-03	0.6%	1.47E-03	1%	3.68E-04	2%	8.76E-05	10%
	Rodlet6	2.34E-04	7%	7.100E-03	0.6%	1.43E-03	1%	3.05E-04	2%	7.70E-05	10%
AFC-2B	Rodlet1	1.51E-04	7%	5.381E-03	0.6%	1.08E-03	1%	2.40E-04	2%	5.36E-05	10%
	Rodlet2	1.96E-04	7%	5.290E-03	0.6%	9.30E-04	1%	2.96E-04	2%	5.93E-05	10%
	Rodlet3	2.24E-04	7%	5.235E-03	0.6%	1.02E-03	1%	3.45E-04	2%	7.03E-05	10%
	Rodlet4	2.87E-04	7%	8.383E-03	0.6%	1.58E-03	1%	4.22E-04	2%	9.24E-05	10%
	Rodlet5	2.69E-04	7%	7.166E-03	0.6%	1.41E-03	1%	3.74E-04	2%	8.60E-05	10%
	Rodlet6	2.26E-04	7%	7.112E-03	0.6%	1.43E-03	1%	3.12E-04	2%	7.79E-05	10%

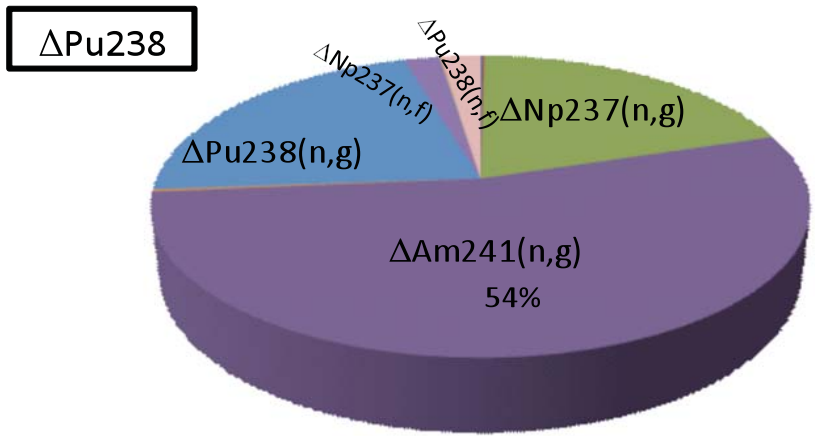

Figure 21. Sensitivity of cross section error to ΔPu238, Density Uncertainty.

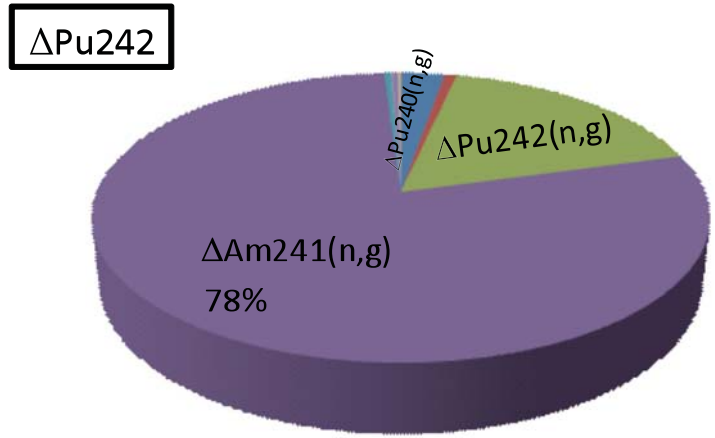

Figure 22. Sensitivity of cross section error to ΔPu242, Density Uncertainty.

Table 4(c). Atomic Density of Am (Cycle 142B EOC).

		Am241 [#/b/cm]	Δ [%]	Am242m [#/b/cm]	Δ [%]	Am243 [#/b/cm]	Δ [%]
AFC-2A	Rodlet1	1.06E-03	3%	1.85E-05	13%	1.71E-05	11%
	Rodlet2	8.90E-04	3%	1.85E-05	13%	1.79E-05	11%
	Rodlet3	9.43E-04	3%	2.07E-05	13%	2.05E-05	11%
	Rodlet4	1.29E-03	3%	2.90E-05	13%	2.83E-05	11%
	Rodlet5	1.39E-03	3%	3.03E-05	13%	2.86E-05	11%
	Rodlet6	1.47E-03	3%	2.73E-05	13%	2.53E-05	11%
AFC-2B	Rodlet1	1.02E-03	3%	1.80E-05	13%	1.68E-05	11%
	Rodlet2	8.81E-04	3%	1.83E-05	13%	1.79E-05	11%
	Rodlet3	9.19E-04	3%	2.16E-05	13%	2.03E-05	11%
	Rodlet4	1.34E-03	3%	3.02E-05	13%	2.96E-05	11%
	Rodlet5	1.34E-03	3%	2.92E-05	13%	2.78E-05	11%
	Rodlet6	1.48E-03	3%	2.80E-05	13%	2.58E-05	11%

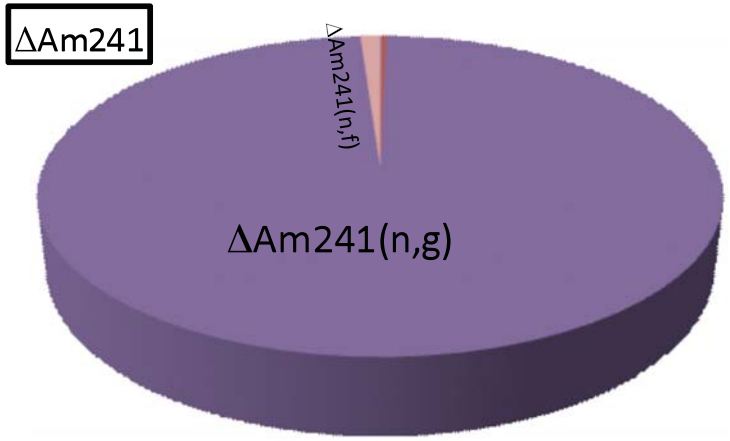

Figure 23. Sensitivity of cross section error to DAm241, Density Uncertainty.

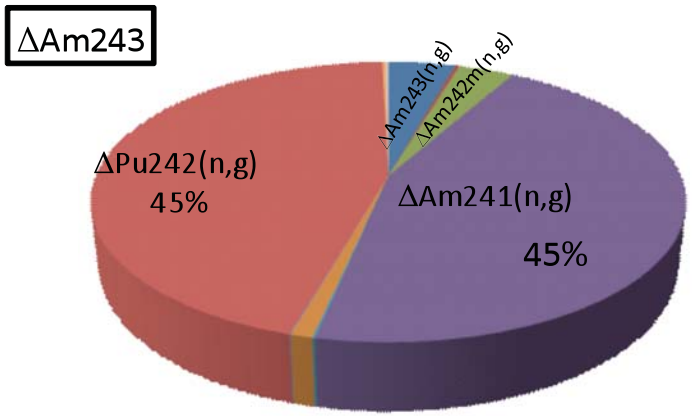

Figure 24. Sensitivity of cross section error to DAm243, Density Uncertainty.

Table 4(d). Atomic Density (Cycle 142B EOC).

		Cm242 [#/b/cm]	Δ [%]	Cm243 [#/b/cm]	Δ [%]	Cm244 [#/b/cm]	Δ [%]
AFC-2A	Rodlet1	9.40E-05	14%	1.46E-06	25%	4.90E-06	13%
	Rodlet2	1.15E-04	14%	2.16E-06	25%	6.84E-06	13%
	Rodlet3	1.35E-04	14%	2.70E-06	25%	8.69E-06	13%
	Rodlet4	1.67E-04	14%	3.13E-06	25%	1.14E-05	13%
	Rodlet5	1.68E-04	14%	2.81E-06	25%	1.06E-05	13%
	Rodlet6	1.38E-04	14%	2.21E-06	25%	7.92E-06	13%
AFC-2B	Rodlet1	9.29E-05	14%	1.62E-06	25%	5.10E-06	13%
	Rodlet2	1.17E-04	14%	2.32E-06	25%	7.72E-06	13%
	Rodlet3	1.39E-04	14%	3.12E-06	25%	8.33E-06	13%
	Rodlet4	1.72E-04	14%	3.35E-06	25%	1.19E-05	13%
	Rodlet5	1.64E-04	14%	3.57E-06	25%	1.08E-05	13%
	Rodlet6	1.40E-04	14%	2.26E-06	25%	8.14E-06	13%

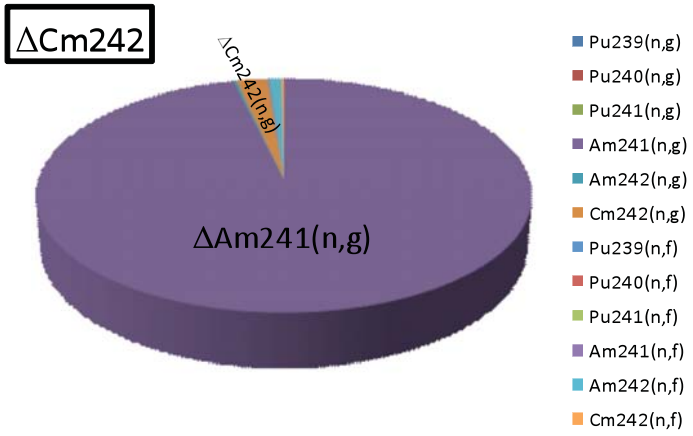

Figure 25. Sensitivity of cross sections error to ΔCm242, Density Uncertainty.

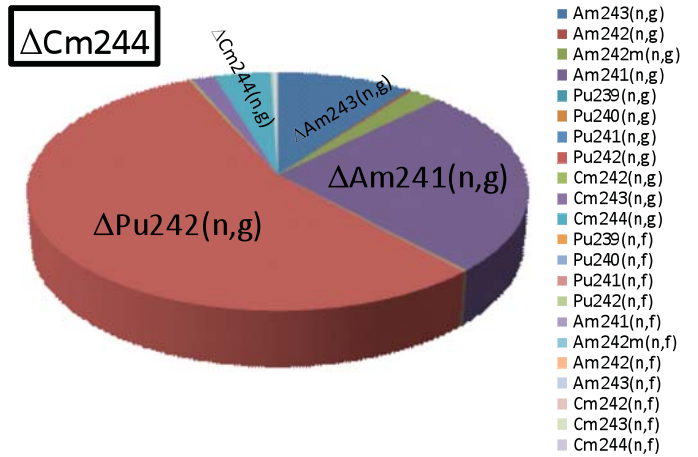

Figure 26. Sensitivity of cross sections error to ΔCm244, Density Uncertainty.

Table 5. Atomic Density of HM (Cycle 140A BOC).

		U235 [#/b/cm]	U236 [#/b/cm]	U238 [#/b/cm]	Np237 [#/b/cm]	Pu238 [#/b/cm]	Pu239 [#/b/cm]	Pu240 [#/b/cm]	Pu241 D[#/b/cm]	Pu242 [#/b/cm]
AFC-2A	Rodlet1	2.099E-02	9.14E-05	1.328E-03	7.05E-04	4.31E-06	6.007E-03	1.19E-03	2.98E-05	2.54E-05
	Rodlet2	1.278E-02	4.76E-04	7.100E-03	6.81E-04	4.48E-06	5.850E-03	1.03E-03	2.65E-05	2.20E-05
	Rodlet3	8.371E-03	3.78E-04	1.098E-02	6.19E-04	4.25E-06	5.853E-03	1.16E-03	2.94E-05	2.51E-05
	Rodlet4	7.672E-03	3.29E-04	6.456E-03	1.22E-03	4.82E-06	8.962E-03	1.63E-03	4.28E-05	3.32E-05
	Rodlet5	8.196E-03	3.33E-04	4.511E-03	9.49E-04	4.36E-06	8.191E-03	1.57E-03	3.88E-05	3.43E-05
	Rodlet6	1.183E-02	3.77E-04	7.449E-04	9.94E-04	8.59E-06	7.703E-03	1.53E-03	3.82E-05	3.38E-05
AFC-2B	Rodlet1	1.945E-02	5.46E-04	1.313E-03	6.46E-04	4.35E-06	5.827E-03	1.15E-03	3.01E-05	2.57E-05
	Rodlet2	1.271E-02	4.80E-04	7.076E-03	6.20E-04	4.44E-06	5.827E-03	1.02E-03	2.63E-05	2.18E-05
	Rodlet3	8.383E-03	3.73E-04	1.100E-02	5.90E-04	4.35E-06	5.790E-03	1.14E-03	3.01E-05	2.57E-05
	Rodlet4	7.901E-03	3.48E-04	6.661E-03	8.70E-04	4.51E-06	9.263E-03	1.69E-03	4.45E-05	3.55E-05
	Rodlet5	8.034E-03	3.90E-04	4.438E-03	8.46E-04	4.46E-06	7.908E-03	1.52E-03	3.97E-05	3.07E-05
	Rodlet6	1.186E-02	3.93E-04	7.467E-04	8.73E-04	8.56E-06	7.733E-03	1.53E-03	3.81E-05	3.37E-05

		Am241 [#/b/cm]	Am242m [#/b/cm]	Am243 [#/b/cm]	Cm242 [#/b/cm]	Cm243 [#/b/cm]	Cm244 [#/b/cm]
AFC-2A	Rodlet1	1.28E-03	0.00E+00	0.00E+00	0.00E+00	0.00E+00	0.00E+00
	Rodlet2	1.16E-03	0.00E+00	0.00E+00	0.00E+00	0.00E+00	0.00E+00
	Rodlet3	1.26E-03	0.00E+00	0.00E+00	0.00E+00	0.00E+00	0.00E+00
	Rodlet4	1.69E-03	0.00E+00	0.00E+00	0.00E+00	0.00E+00	0.00E+00
	Rodlet5	1.79E-03	0.00E+00	0.00E+00	0.00E+00	0.00E+00	0.00E+00
	Rodlet6	1.80E-03	0.00E+00	0.00E+00	0.00E+00	0.00E+00	0.00E+00
AFC-2B	Rodlet1	1.24E-03	0.00E+00	0.00E+00	0.00E+00	0.00E+00	0.00E+00
	Rodlet2	1.16E-03	0.00E+00	0.00E+00	0.00E+00	0.00E+00	0.00E+00
	Rodlet3	1.25E-03	0.00E+00	0.00E+00	0.00E+00	0.00E+00	0.00E+00
	Rodlet4	1.75E-03	0.00E+00	0.00E+00	0.00E+00	0.00E+00	0.00E+00
	Rodlet5	1.73E-03	0.00E+00	0.00E+00	0.00E+00	0.00E+00	0.00E+00
	Rodlet6	1.81E-03	0.00E+00	0.00E+00	0.00E+00	0.00E+00	0.00E+00

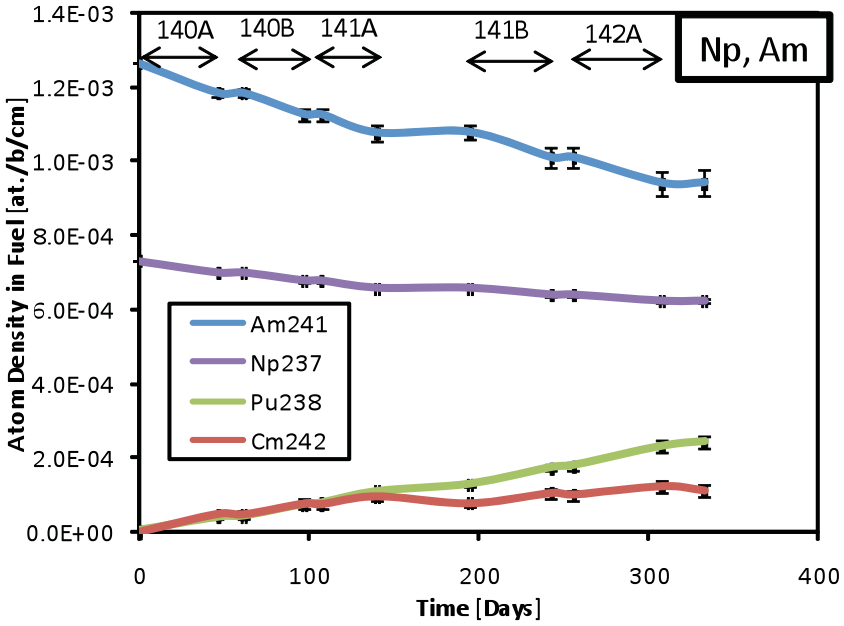

(a) Np-237, Am-241 transmutation and their by-products

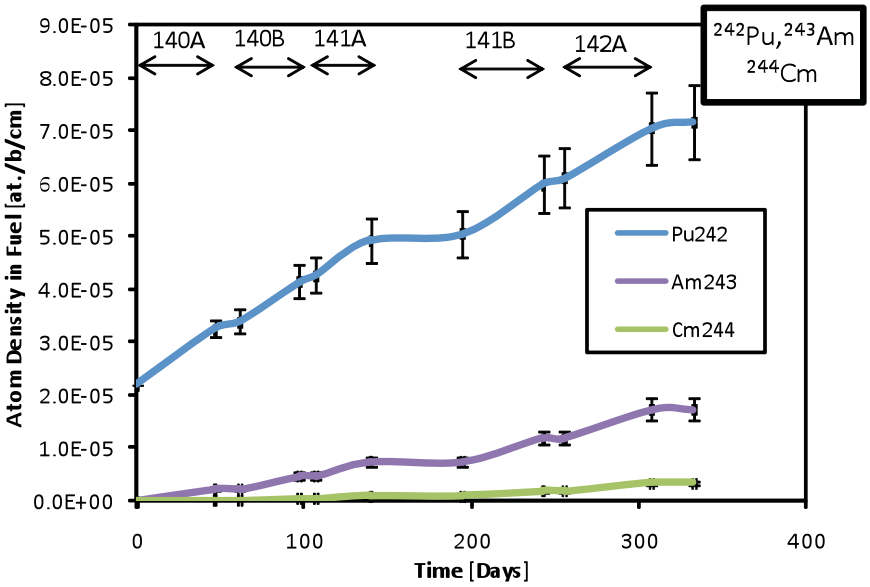

(b) Pu-242, Am-243 transmutation and their by-products

Figure 27. Time dependent HM depletion and buildup (AFC-2A rodlet 3).

3.2.2 HM elemental and isotope composition

Based on the nuclides density provided in previous section, elemental density (Table 6), elemental composition (Table 7) and isotope composition (Table 8) are calculated with uncertainty. Sensitivity of elemental density and composition uncertainty is shown in Figure 28. We can visually evaluate the importance of each cross-section error to the final composition.

Uncertainty of the density of element A consists of isotopes A1, A2, A3… is described as following,

$$\Delta N_A = \sqrt{\Delta N_{A1}{}^2 + \Delta N_{A2}{}^2 + \Delta N_{A3}{}^2 \ldots} \qquad \text{(Eq. 7)}$$

Uncertainty of the elemental composition consists of elements A, B, C … is described as following,

$$R_A \equiv \frac{N_A}{N_A + N_B + N_C + \ldots}$$

$$\Delta R_A = \sqrt{\left(\frac{\partial R_A}{\partial N_A}\Delta N_A\right)^2 + \left(\frac{\partial R_A}{\partial N_B}\Delta N_B\right)^2 + \left(\frac{\partial R_A}{\partial N_c}\Delta N_c\right)^2 + \ldots}$$

$$= \sqrt{\left(\frac{N_B + N_c + \ldots}{(N_A + N_B + N_c + \ldots)^2}\Delta N_A\right)^2 + \left(\frac{-N_A}{(N_A + N_B + N_c + \ldots)^2}\Delta N_B\right)^2 + \left(\frac{-N_A}{(N_A + N_B + N_c + \ldots)^2}\Delta N_c\right)^2 + \ldots} \qquad \text{(Eq. 8)}$$

Uncertainty of the isotopic composition of element A consists of isotopes A1, A2, A3 … is described as following,

$$I_{A1} \equiv \frac{N_{A1}}{N_{A1} + N_{A2} + N_{A3} + \ldots}$$

$$\Delta I_{A1} = \sqrt{\left(\frac{\partial I_{A1}}{\partial N_{A1}}\Delta N_{A1}\right)^2 + \left(\frac{\partial I_{A1}}{\partial N_{A2}}\Delta N_{A2}\right)^2 + \left(\frac{\partial I_{A1}}{\partial N_{A3}}\Delta N_{A3}\right)^2 + \ldots}$$

$$= \sqrt{\left(\frac{N_{A2} + N_{A3} + \ldots}{N_A{}^2}\Delta N_{A1}\right)^2 + \left(\frac{-N_{A1}}{N_A{}^2}\Delta N_{A2}\right)^2 + \left(\frac{-N_{A1}}{N_A{}^2}\Delta N_{A3}\right)^2 + \ldots} \qquad \text{(Eq. 9)}$$

Table 6. HM Elemental Density (Cycle 142B EOC).

		U [#/b/cm]	Δ [%]	Np [#/b/cm]	Δ [%]	Pu [#/b/cm]	Δ [%]	Am [#/b/cm]	Δ [%]	Cm [#/b/cm]	Δ [%]
AFC-2A	Rodlet1	2.158E-02	0.1%	7.05E-04	0.9%	7.13E-03	0.5%	1.09E-03	3%	1.0E-04	13%
	Rodlet2	2.036E-02	0.1%	6.81E-04	0.9%	6.82E-03	0.6%	9.26E-04	3%	1.2E-04	13%
	Rodlet3	1.973E-02	0.1%	6.19E-04	0.9%	6.97E-03	0.5%	9.84E-04	3%	1.5E-04	13%
	Rodlet4	1.446E-02	0.1%	1.22E-03	0.9%	1.05E-02	0.6%	1.35E-03	3%	1.8E-04	13%
	Rodlet5	1.304E-02	0.1%	9.49E-04	0.9%	9.65E-03	0.5%	1.44E-03	3%	1.8E-04	13%
	Rodlet6	1.295E-02	0.1%	9.94E-04	0.9%	9.14E-03	0.5%	1.53E-03	3%	1.5E-04	13%
AFC-2B	Rodlet1	2.131E-02	0.1%	6.46E-04	0.9%	6.90E-03	0.5%	1.06E-03	3%	1.0E-04	13%
	Rodlet2	2.027E-02	0.1%	6.20E-04	0.9%	6.77E-03	0.5%	9.17E-04	3%	1.3E-04	13%
	Rodlet3	1.976E-02	0.1%	5.90E-04	0.9%	6.89E-03	0.6%	9.61E-04	3%	1.5E-04	13%
	Rodlet4	1.491E-02	0.1%	8.70E-04	0.9%	1.08E-02	0.5%	1.40E-03	3%	1.9E-04	13%
	Rodlet5	1.286E-02	0.1%	8.46E-04	0.9%	9.30E-03	0.5%	1.39E-03	3%	1.8E-04	13%
	Rodlet6	1.300E-02	0.1%	8.73E-04	0.9%	9.16E-03	0.5%	1.53E-03	3%	1.5E-04	13%

Table 7. HM Elemental Composition (Cycle 142B EOC).

		U [at. ratio]	Δ [%]	Np [at. ratio]	Δ [%]	Pu [at. ratio]	Δ [%]	Am [at. ratio]	Δ [%]	Cm [at. ratio]	Δ [%]
AFC-2A	Rodlet1	7.051E-01	0.2%	2.30E-02	1%	2.330E-01	0.4%	3.57E-02	3%	3.3E-03	13%
	Rodlet2	7.041E-01	0.2%	2.35E-02	1%	2.360E-01	0.4%	3.20E-02	3%	4.3E-03	13%
	Rodlet3	6.936E-01	0.2%	2.18E-02	1%	2.449E-01	0.4%	3.46E-02	3%	5.2E-03	12%
	Rodlet4	5.220E-01	0.3%	4.39E-02	1%	3.787E-01	0.4%	4.88E-02	3%	6.5E-03	12%
	Rodlet5	5.161E-01	0.3%	3.75E-02	1%	3.820E-01	0.4%	5.72E-02	3%	7.2E-03	13%
	Rodlet6	5.230E-01	0.3%	4.01E-02	1%	3.693E-01	0.4%	6.16E-02	3%	6.0E-03	13%
AFC-2B	Rodlet1	7.100E-01	0.2%	2.15E-02	1%	2.299E-01	0.4%	3.52E-02	3%	3.3E-03	13%
	Rodlet2	7.061E-01	0.2%	2.16E-02	1%	2.359E-01	0.4%	3.20E-02	3%	4.4E-03	12%
	Rodlet3	6.968E-01	0.2%	2.08E-02	1%	2.431E-01	0.4%	3.39E-02	3%	5.3E-03	13%
	Rodlet4	5.301E-01	0.3%	3.09E-02	1%	3.826E-01	0.4%	4.98E-02	3%	6.7E-03	12%
	Rodlet5	5.232E-01	0.3%	3.44E-02	1%	3.785E-01	0.4%	5.66E-02	3%	7.3E-03	12%
	Rodlet6	5.261E-01	0.3%	3.53E-02	1%	3.707E-01	0.4%	6.19E-02	3%	6.1E-03	13%

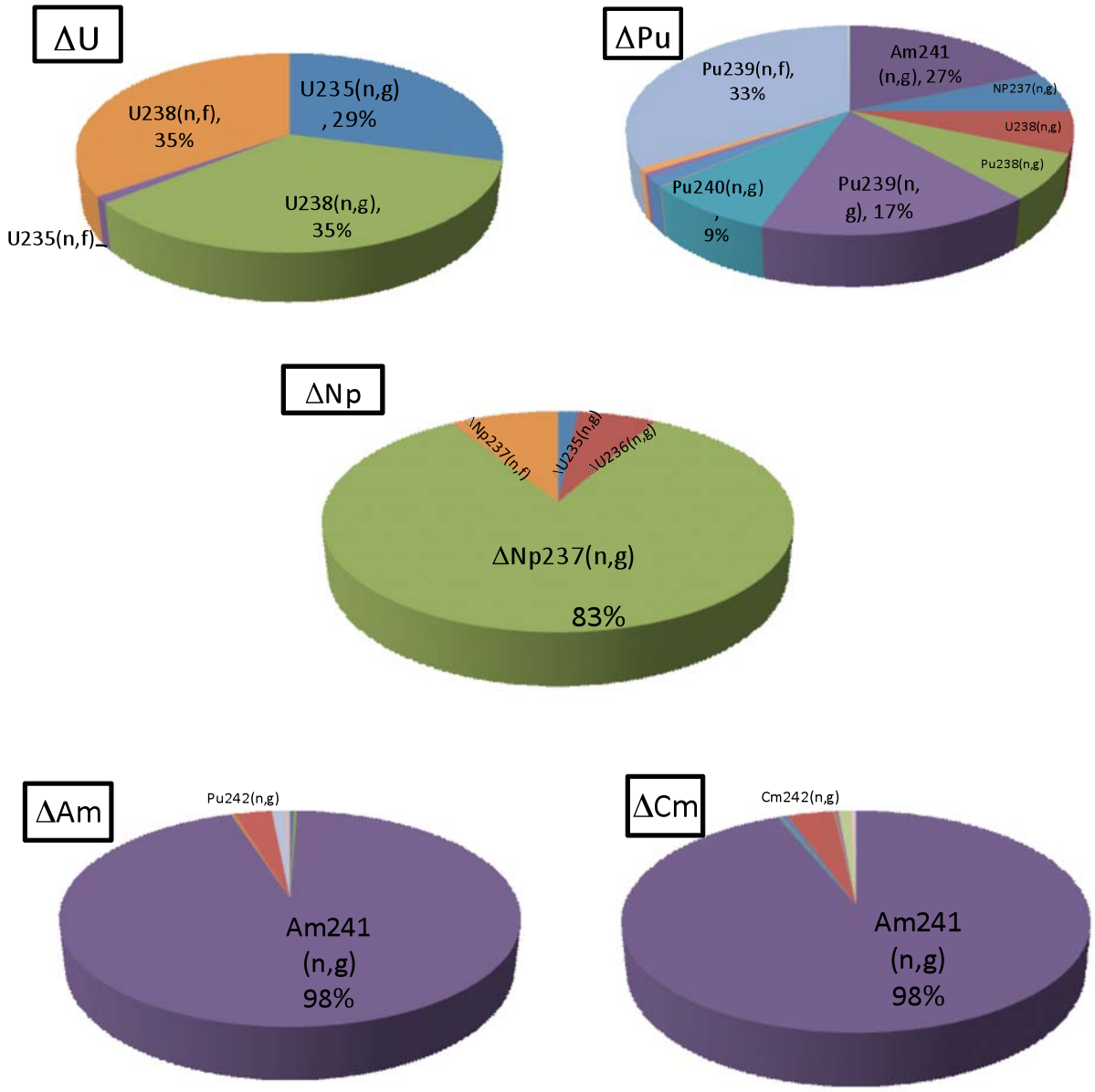

Figure 28. Sensitivity of cross section error to Element Composition Uncertainty (AFC 2A Rodlet 3).

Table 8(a). Isotope Composition of U (Cycle 142B EOC).

		U235 [at. ratio]	Δ [%]	U236 [at. ratio]	Δ [%]	U238 [at. ratio]	Δ [%]
AFC-2A	Rodlet1	9.131E-01	0.02%	2.53E-02	1%	6.152E-02	0.10%
	Rodlet2	6.278E-01	0.04%	2.34E-02	1%	3.488E-01	0.07%
	Rodlet3	4.243E-01	0.06%	1.92E-02	1%	5.565E-01	0.05%
	Rodlet4	5.307E-01	0.05%	2.28E-02	1%	4.466E-01	0.06%
	Rodlet5	6.285E-01	0.04%	2.56E-02	1%	3.459E-01	0.07%
	Rodlet6	9.134E-01	0.03%	2.91E-02	1%	5.751E-02	0.10%
AFC-2B	Rodlet1	9.128E-01	0.02%	2.56E-02	1%	6.162E-02	0.10%
	Rodlet2	6.272E-01	0.04%	2.37E-02	1%	3.492E-01	0.07%
	Rodlet3	4.243E-01	0.06%	1.89E-02	1%	5.568E-01	0.05%
	Rodlet4	5.299E-01	0.05%	2.34E-02	1%	4.467E-01	0.06%
	Rodlet5	6.246E-01	0.05%	3.03E-02	1%	3.450E-01	0.07%
	Rodlet6	9.123E-01	0.03%	3.02E-02	1%	5.744E-02	0.10%

Table 8(b). Isotope Composition of Pu (Cycle 142B EOC).

		Pu238 [at. ratio]	Δ [%]	Pu239 [at. ratio]	Δ [%]	Pu240 [at. ratio]	Δ [%]	Pu241 D [at. ratio]	Δ [%]	Pu242 [at. ratio]	Δ [%]
AFC-2A	Rodlet1	2.158E-02	7%	7.821E-01	0.3%	1.558E-01	0.9%	3.292E-02	2%	7.61E-03	10%
	Rodlet2	2.981E-02	6%	7.813E-01	0.3%	1.377E-01	0.9%	4.253E-02	2%	8.70E-03	10%
	Rodlet3	3.166E-02	6%	7.609E-01	0.3%	1.499E-01	0.9%	4.772E-02	2%	9.82E-03	10%
	Rodlet4	3.137E-02	6%	7.770E-01	0.3%	1.457E-01	0.9%	3.779E-02	2%	8.18E-03	10%
	Rodlet5	2.908E-02	6%	7.719E-01	0.3%	1.518E-01	0.9%	3.817E-02	2%	9.07E-03	10%
	Rodlet6	2.556E-02	6%	7.764E-01	0.3%	1.563E-01	0.9%	3.335E-02	2%	8.42E-03	10%
AFC-2B	Rodlet1	2.184E-02	7%	7.797E-01	0.3%	1.559E-01	0.9%	3.473E-02	2%	7.77E-03	10%
	Rodlet2	2.890E-02	6%	7.812E-01	0.3%	1.374E-01	0.9%	4.376E-02	2%	8.76E-03	10%
	Rodlet3	3.242E-02	6%	7.595E-01	0.3%	1.478E-01	0.9%	5.007E-02	2%	1.02E-02	10%
	Rodlet4	2.663E-02	6%	7.790E-01	0.3%	1.465E-01	0.9%	3.923E-02	2%	8.58E-03	10%
	Rodlet5	2.891E-02	6%	7.702E-01	0.3%	1.514E-01	0.9%	4.023E-02	2%	9.24E-03	10%
	Rodlet6	2.464E-02	6%	7.764E-01	0.3%	1.564E-01	0.9%	3.402E-02	2%	8.50E-03	10%

Table 8(c). Isotope Composition of Am (Cycle 142B EOC).

		Am241 [at. ratio]	Δ [%]	Am242m [at. ratio]	Δ [%]	Am243 [at. ratio]	Δ [%]
AFC-2A	Rodlet1	9.674E-01	0.3%	1.70E-02	13%	1.57E-02	13%
	Rodlet2	9.608E-01	0.4%	1.99E-02	13%	1.93E-02	13%
	Rodlet3	9.582E-01	0.4%	2.10E-02	13%	2.08E-02	13%
	Rodlet4	9.576E-01	0.4%	2.15E-02	13%	2.09E-02	13%
	Rodlet5	9.593E-01	0.4%	2.10E-02	13%	1.98E-02	13%
	Rodlet6	9.655E-01	0.3%	1.79E-02	13%	1.66E-02	13%
AFC-2B	Rodlet1	9.670E-01	0.3%	1.70E-02	13%	1.59E-02	13%
	Rodlet2	9.605E-01	0.4%	2.00E-02	13%	1.95E-02	13%
	Rodlet3	9.563E-01	0.4%	2.25E-02	13%	2.11E-02	13%
	Rodlet4	9.573E-01	0.4%	2.16E-02	13%	2.12E-02	13%
	Rodlet5	9.590E-01	0.4%	2.10E-02	13%	2.00E-02	13%
	Rodlet6	9.648E-01	0.3%	1.83E-02	13%	1.69E-02	13%

Table 8(d). Isotope Composition of Cm (Cycle 142B EOC).

		Cm242 [at. ratio]	Δ [%]	Cm243 [at. ratio]	Δ [%]	Cm244 [at. ratio]	Δ [%]
AFC-2A	Rodlet1	9.366E-01	1.2%	1.46E-02	28%	4.88E-02	18%
	Rodlet2	9.275E-01	1.3%	1.74E-02	27%	5.51E-02	18%
	Rodlet3	9.223E-01	1.4%	1.84E-02	27%	5.93E-02	18%
	Rodlet4	9.197E-01	1.5%	1.73E-02	27%	6.31E-02	18%
	Rodlet5	9.262E-01	1.4%	1.55E-02	28%	5.83E-02	18%
	Rodlet6	9.318E-01	1.2%	1.49E-02	28%	5.34E-02	18%
AFC-2B	Rodlet1	9.325E-01	1.2%	1.63E-02	28%	5.12E-02	18%
	Rodlet2	9.207E-01	1.5%	1.83E-02	27%	6.10E-02	18%
	Rodlet3	9.241E-01	1.4%	2.07E-02	27%	5.52E-02	18%
	Rodlet4	9.187E-01	1.5%	1.79E-02	27%	6.34E-02	18%
	Rodlet5	9.197E-01	1.5%	2.00E-02	27%	6.03E-02	18%
	Rodlet6	9.307E-01	1.3%	1.51E-02	28%	5.43E-02	18%

Burnup and its uncertainty

Based on the nuclides density provided in previous section, burnup (Table 9) is calculated with uncertainty. Sensitivity of cross section error to burnup uncertainty is shown in Figure 29. We can visually evaluate the importance of each cross-section error to burnup.

Uncertainty of Burnup is described as following,

$$BU[FIMA] = \frac{N_{HM_{BOC}} - N_{HM_{EOC}}}{N_{HM_{BOC}}}$$

$$\Delta BU = \sqrt{\left(\frac{\partial BU}{\partial N_{HM_{EOC}}}\Delta N_{HM_{EOC}}\right)^2} = \left|\frac{\Delta N_{HM_{EOC}}}{N_{HM_{EOC}}}\right| \qquad \text{(Eq. 10)}$$

In Table 9, burnups at the end of cycle 142B are listed. Burnup values of each fuel pins are varied from 3.6% to 4.6%, because of the difference in neutron fluence and fissile nuclide component. As for the uncertainty of burnup in each fuel pin, it is not simply proportional to the burnup. For example, though rodlet1 has much smaller burnup than others, the uncertainty is much larger than rodlet 2 and 3. Comparing rodlet1 with rodlet3, fuel composition is the same except the enrichment of uranium, 93% EU in rodlet1 and 55% in rodlet3. Since U-235 cross section, especially capture cross section error has big sensitivity to U-236 and Np-237 accumulation, this difference affects the uncertainty of burnup in each fuel pin. As shown in Figure 29(a) and Figure 29(b), the sensitivity of cross section error to burnup uncertainty in rodlet1 and rodlet3 can be visually confirmed and major difference is caused by the difference of U-235(n,g) error. Comparing rodlet1 with rodlet6, composition of Pu, Am, Np and the enrichment of U is increased in rodlet 6. As shown in Figure 29(a) and Figure 29(c), the sensitivity of cross section error to burnup uncertainty in rodlet1 and rodlet6 can be visually confirmed and the major difference is caused by the increasing Am-241(n,g) error.

Table 9. BURNUP (Cycle 142B EOC).

		FIMA [DHM/HMin]	Δ [%]
AFC-2A	Rodlet1	3.625E-02	5%
	Rodlet2	4.227E-02	4%
	Rodlet3	3.919E-02	5%
	Rodlet4	4.341E-02	7%
	Rodlet5	4.405E-02	7%
	Rodlet6	4.112E-02	7%
AFC-2B	Rodlet1	3.846E-02	5%
	Rodlet2	4.299E-02	4%
	Rodlet3	4.048E-02	5%
	Rodlet4	4.539E-02	6%
	Rodlet5	4.604E-02	6%
	Rodlet6	4.241E-02	7%

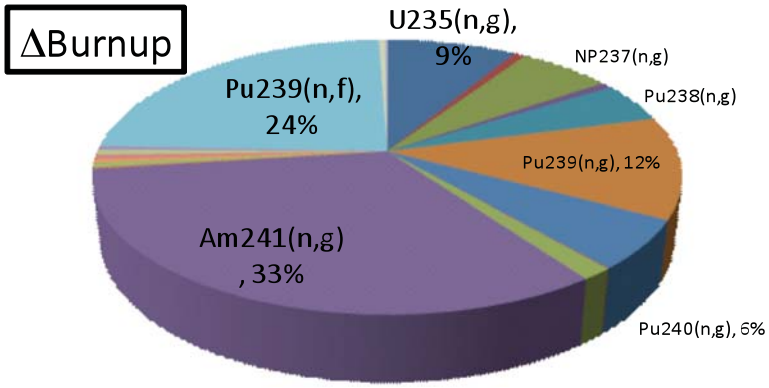

(a) AFC-2A rodlet 1 (U-20Pu-3Am-2Np-15Zr, 93%EU)

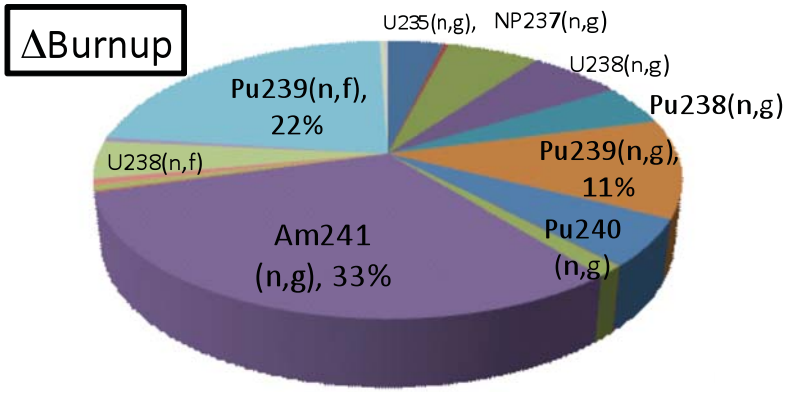

(b) AFC-2A rodlet 3 (U-20Pu-3Am-2Np-15Zr-1.0RE, 55%EU)

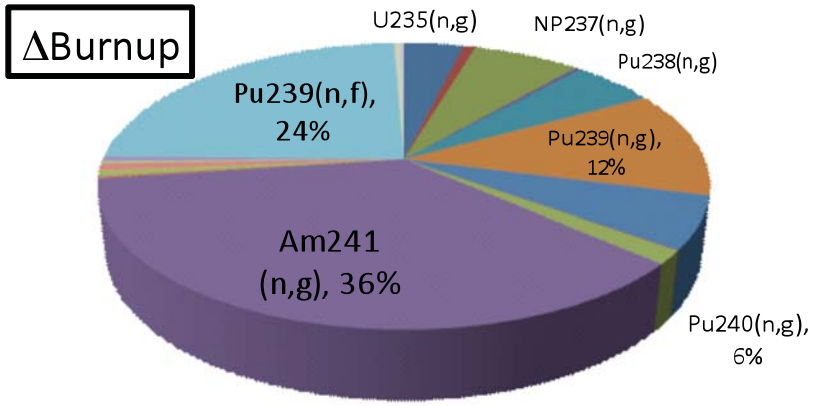

(c) AFC-2A rodlet 6 (U-30Pu-5Am-3Np-1.0RE-15Zr, 93%EU)

Figure 29. Sensitivity of Cross-section Error to Burnup Uncertainty.

4. CONCLUSION

Uncertainty analysis relating to calculations for AFC-2A and AFC-2B has been performed. The methodology to treat the nuclear cross section covariance and global uncertainty in depletion and buildup calculations was established by addition to current MCWO code system with interface of ORIGEN Library. This uncertainty analysis methodology was applied for AFC-2A and AFC-2B fuel pin irradiation, and uncertainties of HM density, elemental composition, isotope composition and burnup are calculated. As a result, the sensitivity of cross section errors are evaluated coupling with original as-run calculations by MCWO, and the importance of cross section error to the final output is evaluated by sensitivity analysis. This methodology and results can provide productive information to PIE experimentalists to discuss the discrepancy between calculations and experiments in AFCI program. And also, the uncertainty information can be utilized by the safety evaluation, validation of code and nuclear data, and their improvement.

5. ACKNOWLEDGEMENT

To perform the present work, we got lots of productive comment from Fuel and PIE engineers, Dr. Steve Hayes, Mr. Jon Carmack, Dr. Bruce Hilton and Dr. Irina Glagolenko. For processing the error data of Low-Fidelity Covariance by ERRORJ, I achieved big help from Dr. Go Chiba, JAEA, and Scientists in Brookhaven National Laboratory. Special Thanks to Ms. Misti Lillo for her support of calculation environment and Mr. Richard G. Ambrosek for his technical proof-read. We would like to express our great gratitude to them.

6. REFERENCES

1. Evaluated Nuclear Data File, http://www.nndc.bnl.gov/exfor/endf00.jsp
2. Japanese Evaluated Nuclear Data Library, http://wwwndc.jaea.go.jp/jendl/jendl.html
3. http://www.nea.fr/html/dbdata/projects/jeffdoc.html
4. http://www.talys.eu/tendl-2008/
5. R.C. Little et al., "Low-Fidelity Covariance Project", Nuclear Data Sheets 109, 2828-2833 (2008). Data can be downloaded from http://www.nndc.bnl.gov/lowfi/
6. H. J. MacLean, D. J. Utterbeck, G. S. Chang, M, A. Lillo, “Advanced Fuel Cycle Initiative AFC-1G, AFC-1H, AFC-2A, and AFC-2B End of FY-08 Irradiation Report,” INL/EXT-08 14829 (2008).
7. S. L. Hayes, “Irradiation of Metalic Fuel with Rare Earth Additions for Actinide Transmutation in the Advanced Test Reactor, Experiment Description for AFC-2A and AFC-2B,” INL/EXT-06 11707 (2007).
8. S. L. Hayes, D. J. Utterbeck, “Project Description Advanced Fuel Cycle Initiative AFC-2A and AFC-2B Experiments,” INL/EXT-07-12388 (2007)
9. INL/EXT-07-12388
10. INL/EXT-07-13021
11. ORNL, “ORIGEN 2.2 Isotope Generation and Depletion Code Matrix Exponential Method,” CCC-371, RSICC(2002).
12. G Chang, “MCWO: Monte Carlo , depletion methodology to Coupling MCNP5 with ORIGEN2,” INL

13. G. Chiba, "ERRORJ : A Code to Process Neutron-nuclide Reaction Cross Section Covariance, Version 2.3, " JAEA-Data/Code 2007-007 (2007).

14. Kosako K. and Yamano N., 'Preparation of a Covariance Processing System for the Evaluated Nuclear Data File, JENDL, (III),' JNC TJ 9440 99-003, Japan Nuclear Cycle Development Institute (1999) [in Japanese].

15. MacFarlane R.E. and Muir D.W., 'The NJOY Nuclear Data Processing System version 91,' LA-12740-M, Los Alamos National Laboratory (1994).

16. Wiarda D., Dunn M.E., el al., 'New Capability for Processing Covariance Data in Resonance Region,' Proc. of Int. Conf. of Reactor Physics (PHYSOR-2006), (CD-ROM) (2006).

17. D. H. Kim, el al., 'Sensitivity and uncertainty analysis on the criticality by an ERRORJ/SUSD3D with JENDL-3.3 covariance data,' Proc. International Conference on Nuclear Data for Science and Technology (2007).

Appendix A

Results of Isolated EFT Model with Boundary Neutron Source ($\Delta\phi$ = 5-10%)

A-1. Results of Isolated EFT Model with Boundary Neutron Source (Δϕ = 5-10%)

Table A-1. Atomic Density (Cycle 142B EOC), Δϕ = 10%.

		U235 [#/b/cm]	Δ [%]	U236 [#/b/cm]	Δ [%]	U238 [#/b/cm]	Δ [%]	Np237 [#/b/cm]	Δ [%]
AFC-2A	Rodlet1	1.946E-02	1%	5.54E-04	9%	1.323E-03	0.2%	6.98E-04	2%
	Rodlet2	1.261E-02	1%	4.82E-04	9%	7.082E-03	0.2%	6.70E-04	2%
	Rodlet3	8.250E-03	1%	3.83E-04	9%	1.094E-02	0.2%	6.08E-04	2%
	Rodlet4	7.570E-03	1%	3.34E-04	9%	6.438E-03	0.2%	1.19E-03	2%
	Rodlet5	8.082E-03	1%	3.38E-04	9%	4.493E-03	0.2%	9.33E-04	2%
	Rodlet6	1.170E-02	1%	3.81E-04	9%	7.407E-04	0.2%	9.74E-04	2%
AFC-2B	Rodlet1	1.924E-02	1%	5.52E-04	9%	1.304E-03	0.2%	6.38E-04	2%
	Rodlet2	1.250E-02	1%	4.88E-04	9%	7.052E-03	0.2%	6.04E-04	2%
	Rodlet3	8.280E-03	1%	3.78E-04	9%	1.097E-02	0.2%	5.79E-04	2%
	Rodlet4	7.793E-03	1%	3.53E-04	9%	6.648E-03	0.2%	8.49E-04	2%
	Rodlet5	7.931E-03	1%	3.95E-04	9%	4.422E-03	0.2%	8.29E-04	2%
	Rodlet6	1.174E-02	1%	3.97E-04	9%	7.492E-04	0.2%	8.56E-04	2%

Table A-2. Atomic Density (Cycle 142B EOC), Δϕ = 10%.

		Pu238 [#/b/cm]	Δ [%]	Pu239 [#/b/cm]	Δ [%]	Pu240 [#/b/cm]	Δ [%]	Pu241 D[#/b/cm]	Δ [%]	Pu242 [#/b/cm]	Δ [%]
AFC-2A	Rodlet1	1.76E-04	7%	5.496E-03	2%	1.10E-03	2%	2.69E-04	9%	6.02E-05	12%
	Rodlet2	2.28E-04	7%	5.277E-03	2%	9.41E-04	2%	3.08E-04	9%	6.30E-05	12%
	Rodlet3	2.48E-04	7%	5.227E-03	2%	1.02E-03	2%	3.81E-04	9%	7.37E-05	12%
	Rodlet4	3.76E-04	7%	8.040E-03	2%	1.51E-03	2%	4.45E-04	9%	9.41E-05	12%
	Rodlet5	3.07E-04	7%	7.371E-03	2%	1.46E-03	2%	3.93E-04	9%	9.15E-05	12%
	Rodlet6	2.65E-04	7%	6.980E-03	2%	1.43E-03	2%	3.37E-04	9%	8.12E-05	12%
AFC-2B	Rodlet1	1.72E-04	7%	5.325E-03	2%	1.04E-03	2%	2.88E-04	9%	5.94E-05	12%
	Rodlet2	2.31E-04	7%	5.215E-03	2%	9.15E-04	2%	3.33E-04	9%	6.46E-05	12%
	Rodlet3	2.43E-04	7%	5.180E-03	2%	1.01E-03	2%	3.74E-04	9%	7.47E-05	12%
	Rodlet4	3.26E-04	7%	8.280E-03	2%	1.55E-03	2%	4.70E-04	9%	1.02E-04	12%
	Rodlet5	3.04E-04	7%	7.076E-03	2%	1.38E-03	2%	4.18E-04	9%	9.37E-05	12%
	Rodlet6	2.52E-04	7%	7.040E-03	2%	1.42E-03	2%	3.40E-04	9%	8.41E-05	12%

Table A-3. Atomic Density (Cycle 142B EOC), Δϕ = 10%.

		Am241 [#/b/cm]	Δ [%]	Am242m [#/b/cm]	Δ [%]	Am243 [#/b/cm]	Δ [%]
AFC-2A	Rodlet1	1.02E-03	5%	1.91E-05	15%	9.64E-06	15%
	Rodlet2	8.53E-04	5%	1.93E-05	15%	1.34E-05	15%
	Rodlet3	9.05E-04	5%	2.16E-05	15%	1.53E-05	15%
	Rodlet4	1.24E-03	5%	3.02E-05	15%	1.78E-05	15%
	Rodlet5	1.35E-03	5%	3.10E-05	15%	1.80E-05	15%
	Rodlet6	1.44E-03	5%	2.80E-05	15%	1.42E-05	15%
AFC-2B	Rodlet1	9.86E-04	5%	1.86E-05	15%	1.05E-05	15%
	Rodlet2	8.34E-04	5%	1.93E-05	15%	1.34E-05	15%
	Rodlet3	8.98E-04	5%	2.21E-05	15%	1.43E-05	15%
	Rodlet4	1.28E-03	5%	3.17E-05	15%	1.81E-05	15%
	Rodlet5	1.29E-03	5%	3.04E-05	15%	1.51E-05	15%
	Rodlet6	1.44E-03	5%	2.86E-05	15%	1.29E-05	15%

Table A-4. Atomic Density (Cycle 142B EOC), Δϕ = 10%.

		Cm242 [#/b/cm]	Δ [%]	Cm243 [#/b/cm]	Δ [%]	Cm244 [#/b/cm]	Δ [%]
AFC-2A	Rodlet1	1.05E-04	16%	1.51E-06	25%	2.76E-06	22%
	Rodlet2	1.29E-04	16%	2.25E-06	25%	5.13E-06	22%
	Rodlet3	1.49E-04	16%	2.81E-06	25%	6.50E-06	22%
	Rodlet4	1.86E-04	16%	3.26E-06	25%	7.19E-06	22%
	Rodlet5	1.79E-04	16%	2.88E-06	25%	6.64E-06	22%
	Rodlet6	1.50E-04	16%	2.26E-06	25%	4.44E-06	22%
AFC-2B	Rodlet1	1.07E-04	16%	1.68E-06	25%	3.19E-06	22%
	Rodlet2	1.34E-04	16%	2.45E-06	25%	5.79E-06	22%
	Rodlet3	1.46E-04	16%	3.19E-06	25%	5.87E-06	22%
	Rodlet4	1.97E-04	16%	3.52E-06	25%	7.24E-06	22%
	Rodlet5	1.81E-04	16%	3.71E-06	25%	5.84E-06	22%
	Rodlet6	1.52E-04	16%	2.31E-06	25%	4.06E-06	22%

Table A-5. HM Elemental Density (Cycle 142B EOC), $\Delta\phi$ = 10%.

		U [#/b/cm]	Δ [%]	Np [#/b/cm]	Δ [%]	Pu [#/b/cm]	Δ [%]	Am [#/b/cm]	Δ [%]	Cm [#/b/cm]	Δ [%]
AFC-2A	Rodlet1	2.134E-02	1.1%	6.98E-04	2%	7.10E-03	2%	1.05E-03	5%	1.1E-04	15%
	Rodlet2	2.017E-02	0.8%	6.70E-04	2%	6.82E-03	2%	8.86E-04	5%	1.4E-04	15%
	Rodlet3	1.958E-02	0.6%	6.08E-04	2%	6.95E-03	2%	9.41E-04	5%	1.6E-04	15%
	Rodlet4	1.434E-02	0.7%	1.19E-03	2%	1.05E-02	2%	1.29E-03	5%	2.0E-04	15%
	Rodlet5	1.291E-02	0.8%	9.33E-04	2%	9.62E-03	2%	1.40E-03	5%	1.9E-04	15%
	Rodlet6	1.282E-02	1.2%	9.74E-04	2%	9.09E-03	2%	1.48E-03	5%	1.6E-04	15%
AFC-2B	Rodlet1	2.110E-02	1.1%	6.38E-04	2%	6.88E-03	2%	1.01E-03	5%	1.1E-04	15%
	Rodlet2	2.004E-02	0.8%	6.04E-04	2%	6.76E-03	2%	8.67E-04	5%	1.4E-04	15%
	Rodlet3	1.962E-02	0.6%	5.79E-04	2%	6.88E-03	2%	9.34E-04	5%	1.6E-04	15%
	Rodlet4	1.479E-02	0.7%	8.49E-04	2%	1.07E-02	2%	1.33E-03	5%	2.1E-04	15%
	Rodlet5	1.275E-02	0.8%	8.29E-04	2%	9.27E-03	2%	1.33E-03	5%	1.9E-04	15%
	Rodlet6	1.288E-02	1.2%	8.56E-04	2%	9.13E-03	2%	1.48E-03	5%	1.6E-04	15%

Table A-6. HM Elemental Composition (Cycle 142B EOC), $\Delta\phi$ = 10%.

		U [at. ratio]	Δ [%]	Np [at. ratio]	Δ [%]	Pu [at. ratio]	Δ [%]	Am [at. ratio]	Δ [%]	Cm [at. ratio]	Δ [%]
AFC-2A	Rodlet1	7.042E-01	0.5%	2.30E-02	2%	2.344E-01	1.4%	3.47E-02	5%	3.6E-03	15%
	Rodlet2	7.033E-01	0.5%	2.34E-02	2%	2.377E-01	1.3%	3.09E-02	5%	4.7E-03	15%
	Rodlet3	6.934E-01	0.5%	2.15E-02	2%	2.461E-01	1.2%	3.33E-02	4%	5.6E-03	15%
	Rodlet4	5.219E-01	0.7%	4.32E-02	2%	3.808E-01	1.0%	4.70E-02	4%	7.1E-03	15%
	Rodlet5	5.154E-01	0.8%	3.73E-02	2%	3.839E-01	1.1%	5.59E-02	4%	7.5E-03	15%
	Rodlet6	5.228E-01	0.8%	3.97E-02	2%	3.707E-01	1.2%	6.04E-02	4%	6.4E-03	15%
AFC-2B	Rodlet1	7.092E-01	0.5%	2.15E-02	2%	2.314E-01	1.4%	3.41E-02	5%	3.7E-03	15%
	Rodlet2	7.054E-01	0.5%	2.13E-02	2%	2.379E-01	1.3%	3.05E-02	5%	5.0E-03	15%
	Rodlet3	6.965E-01	0.4%	2.06E-02	2%	2.443E-01	1.2%	3.32E-02	4%	5.5E-03	15%
	Rodlet4	5.301E-01	0.7%	3.04E-02	2%	3.845E-01	1.0%	4.76E-02	4%	7.4E-03	15%
	Rodlet5	5.231E-01	0.8%	3.40E-02	2%	3.805E-01	1.1%	5.46E-02	4%	7.8E-03	15%
	Rodlet6	5.255E-01	0.8%	3.49E-02	2%	3.726E-01	1.2%	6.05E-02	4%	6.5E-03	15%

Table A-7. Isotope Composition (Cycle 142B EOC), Δϕ = 10%.

		U235 [at. ratio]	Δ [%]	U236 [at. ratio]	Δ [%]	U238 [at. ratio]	Δ [%]
AFC-2A	Rodlet1	9.120E-01	0.2%	2.597E-02	8%	6.202E-02	1.2%
	Rodlet2	6.251E-01	0.5%	2.390E-02	8%	3.510E-01	0.8%
	Rodlet3	4.215E-01	0.7%	1.959E-02	8%	5.590E-01	0.6%
	Rodlet4	5.278E-01	0.6%	2.328E-02	8%	4.489E-01	0.7%
	Rodlet5	6.259E-01	0.5%	2.618E-02	8%	3.480E-01	0.8%
	Rodlet6	9.125E-01	0.3%	2.971E-02	8%	5.777E-02	1.2%
AFC-2B	Rodlet1	9.120E-01	0.2%	2.616E-02	8%	6.180E-02	1.2%
	Rodlet2	6.238E-01	0.5%	2.434E-02	8%	3.519E-01	0.8%
	Rodlet3	4.220E-01	0.7%	1.924E-02	8%	5.588E-01	0.6%
	Rodlet4	5.267E-01	0.6%	2.386E-02	8%	4.494E-01	0.7%
	Rodlet5	6.221E-01	0.5%	3.101E-02	8%	3.469E-01	0.8%
	Rodlet6	9.110E-01	0.3%	3.080E-02	8%	5.815E-02	1.2%

Table A-8. Isotope Composition (Cycle 142B EOC), Δϕ = 10%.

		Pu238 [at. ratio]	Δ [%]	Pu239 [at. ratio]	Δ [%]	Pu240 [at. ratio]	Δ [%]	Pu241 D [at. ratio]	Δ [%]	Pu242 [at. ratio]	Δ [%]
AFC-2A	Rodlet1	2.479E-02	7%	7.739E-01	0.6%	1.549E-01	2.2%	3.788E-02	9%	8.48E-03	12%
	Rodlet2	3.351E-02	7%	7.740E-01	0.7%	1.381E-01	2.2%	4.523E-02	9%	9.24E-03	12%
	Rodlet3	3.565E-02	7%	7.524E-01	0.8%	1.465E-01	2.2%	5.484E-02	9%	1.06E-02	12%
	Rodlet4	3.597E-02	7%	7.683E-01	0.7%	1.442E-01	2.2%	4.256E-02	9%	8.99E-03	12%
	Rodlet5	3.189E-02	7%	7.662E-01	0.7%	1.515E-01	2.2%	4.090E-02	9%	9.51E-03	12%
	Rodlet6	2.916E-02	7%	7.676E-01	0.7%	1.572E-01	2.1%	3.709E-02	9%	8.93E-03	12%
AFC-2B	Rodlet1	2.495E-02	7%	7.734E-01	0.7%	1.511E-01	2.2%	4.185E-02	9%	8.63E-03	12%
	Rodlet2	3.416E-02	7%	7.716E-01	0.7%	1.354E-01	2.2%	4.929E-02	9%	9.55E-03	12%
	Rodlet3	3.523E-02	7%	7.525E-01	0.8%	1.471E-01	2.2%	5.435E-02	9%	1.08E-02	12%
	Rodlet4	3.041E-02	7%	7.716E-01	0.7%	1.447E-01	2.2%	4.377E-02	9%	9.48E-03	12%
	Rodlet5	3.277E-02	7%	7.631E-01	0.7%	1.490E-01	2.2%	4.504E-02	9%	1.01E-02	12%
	Rodlet6	2.757E-02	7%	7.707E-01	0.7%	1.554E-01	2.2%	3.718E-02	9%	9.21E-03	12%

Table A-9. Isotope Composition (Cycle 142B EOC), Δϕ = 10%.

		Am241 [at. ratio]	Δ [%]	Am242m [at. ratio]	Δ [%]	Am243 [at. ratio]	Δ [%]
AFC-2A	Rodlet1	9.727E-01	0.3%	1.82E-02	16%	9.15E-03	16%
	Rodlet2	9.631E-01	0.4%	2.17E-02	16%	1.51E-02	16%
	Rodlet3	9.608E-01	0.5%	2.29E-02	16%	1.63E-02	16%
	Rodlet4	9.628E-01	0.4%	2.34E-02	16%	1.38E-02	16%
	Rodlet5	9.650E-01	0.4%	2.22E-02	16%	1.28E-02	16%
	Rodlet6	9.715E-01	0.3%	1.89E-02	16%	9.61E-03	16%
AFC-2B	Rodlet1	9.713E-01	0.3%	1.84E-02	16%	1.04E-02	16%
	Rodlet2	9.622E-01	0.5%	2.23E-02	16%	1.55E-02	16%
	Rodlet3	9.610E-01	0.5%	2.37E-02	16%	1.53E-02	16%
	Rodlet4	9.625E-01	0.5%	2.39E-02	16%	1.36E-02	16%
	Rodlet5	9.658E-01	0.4%	2.28E-02	16%	1.13E-02	16%
	Rodlet6	9.720E-01	0.3%	1.93E-02	16%	8.69E-03	16%

Table A-10. Isotope Composition (Cycle 142B EOC), Δϕ = 10%

		Cm242 [at. ratio]	Δ [%]	Cm243 [at. ratio]	Δ [%]	Cm244 [at. ratio]	Δ [%]
AFC-2A	Rodlet1	9.610E-01	0.9%	1.38E-02	29%	2.52E-02	26%
	Rodlet2	9.458E-01	1.3%	1.65E-02	29%	3.77E-02	26%
	Rodlet3	9.414E-01	1.4%	1.77E-02	29%	4.09E-02	26%
	Rodlet4	9.468E-01	1.2%	1.66E-02	29%	3.66E-02	26%
	Rodlet5	9.495E-01	1.2%	1.53E-02	29%	3.52E-02	26%
	Rodlet6	9.574E-01	1.0%	1.44E-02	29%	2.83E-02	26%
AFC-2B	Rodlet1	9.563E-01	1.0%	1.51E-02	29%	2.86E-02	26%
	Rodlet2	9.422E-01	1.3%	1.72E-02	29%	4.06E-02	26%
	Rodlet3	9.415E-01	1.3%	2.06E-02	28%	3.79E-02	26%
	Rodlet4	9.482E-01	1.2%	1.69E-02	29%	3.49E-02	26%
	Rodlet5	9.500E-01	1.1%	1.94E-02	29%	3.06E-02	26%
	Rodlet6	9.597E-01	0.9%	1.46E-02	29%	2.57E-02	26%

Table A-11. BURNUP (Cycle 142B EOC), $\Delta\phi$ = 10%.

		FIMA [ΔHM/HMin]	Δ [%]
AFC-2A	Rodlet1	4.621E-02	19%
	Rodlet2	4.975E-02	13%
	Rodlet3	4.642E-02	12%
	Rodlet4	5.081E-02	14%
	Rodlet5	5.197E-02	14%
	Rodlet6	5.033E-02	17%
AFC-2B	Rodlet1	4.697E-02	18%
	Rodlet2	5.257E-02	12%
	Rodlet3	4.640E-02	12%
	Rodlet4	5.286E-02	13%
	Rodlet5	5.425E-02	14%
	Rodlet6	5.003E-02	17%

Appendix B

Cross Section and Fission Yield Error of RE Nuclide

B-1. Results of Isolated EFT Model with Boundary Neutron Source ($\Delta\phi$ = 5-10%)

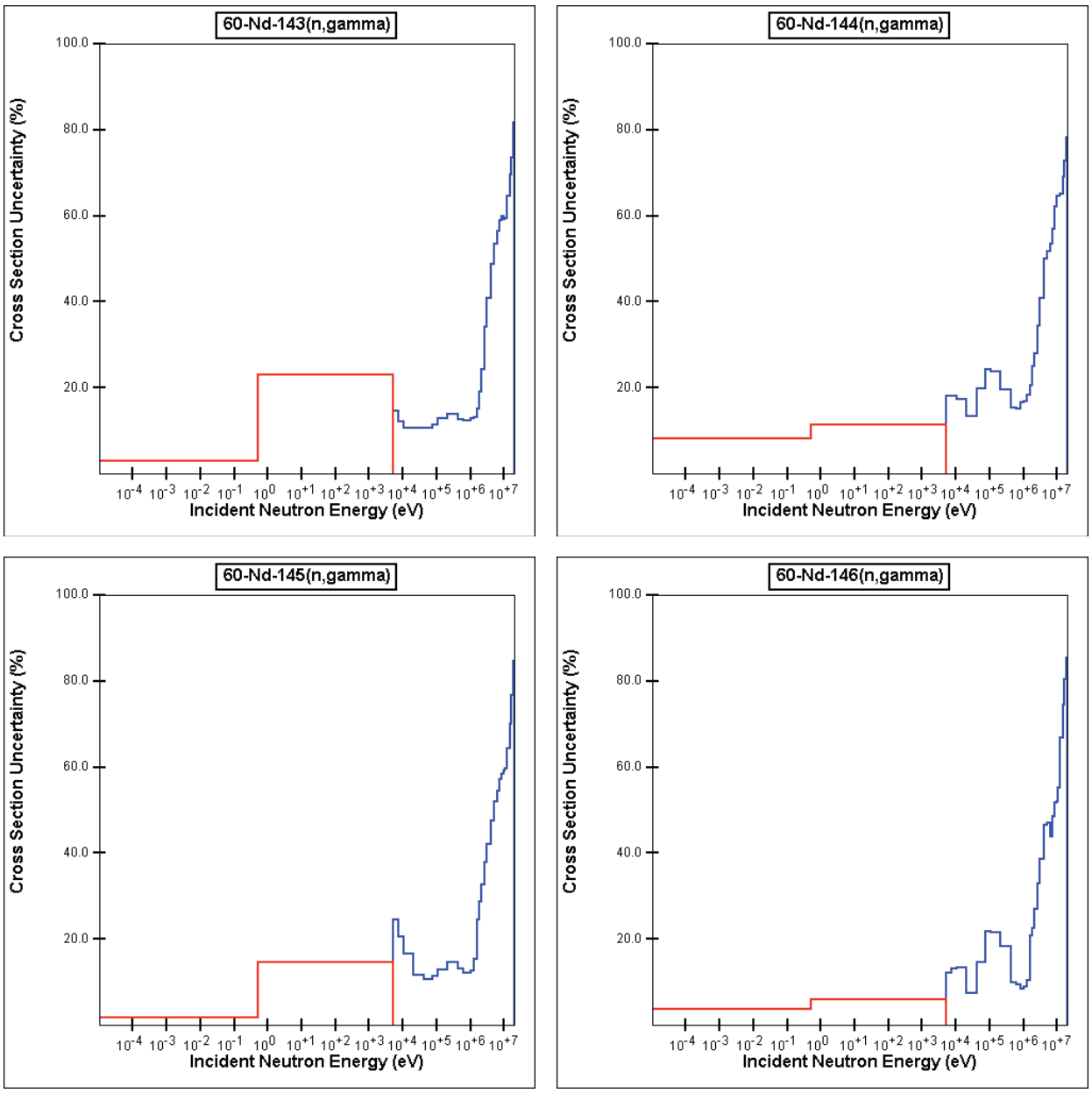

FigureB-1. Capture cross section error of Nd isotope (Data is derived from Low-Fidelity Covariance[5]).

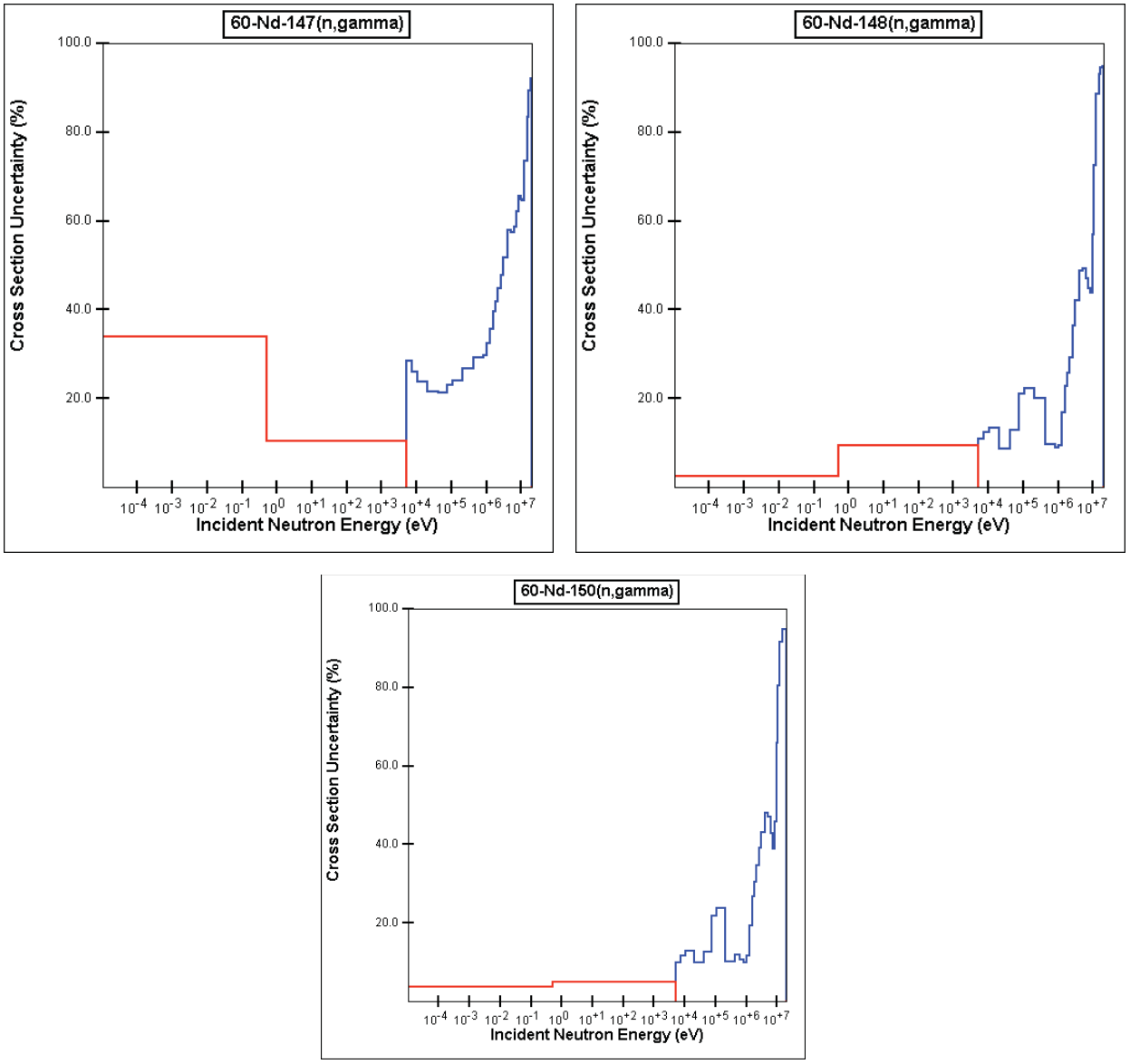

FigureB-2. Capture cross section error of Nd isotope (Data is derived from Low-Fidelity Covariance[5]).

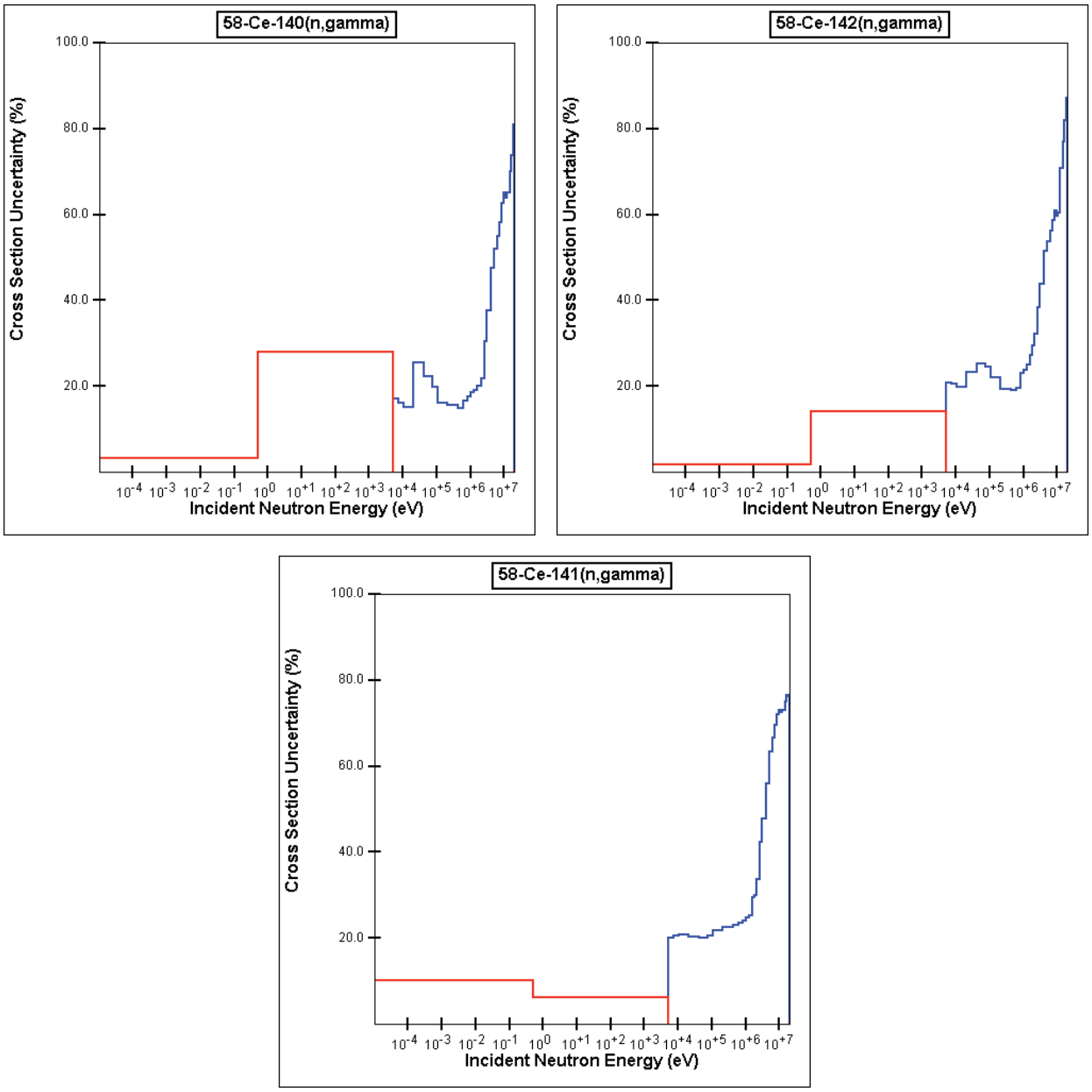

FigureB-3. Capture cross section error of Ce isotope (Data is derived from Low-Fidelity Covariance5).

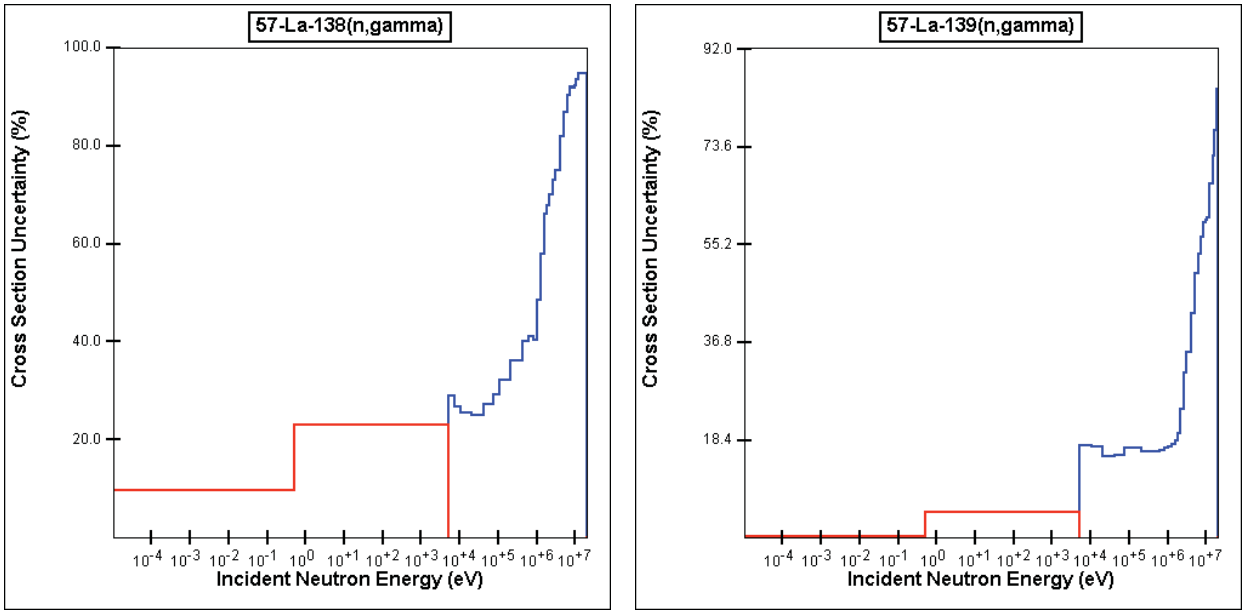

FigureB-4. Capture cross section error of La isotope (Data is derived from Low-Fidelity Covariance5).

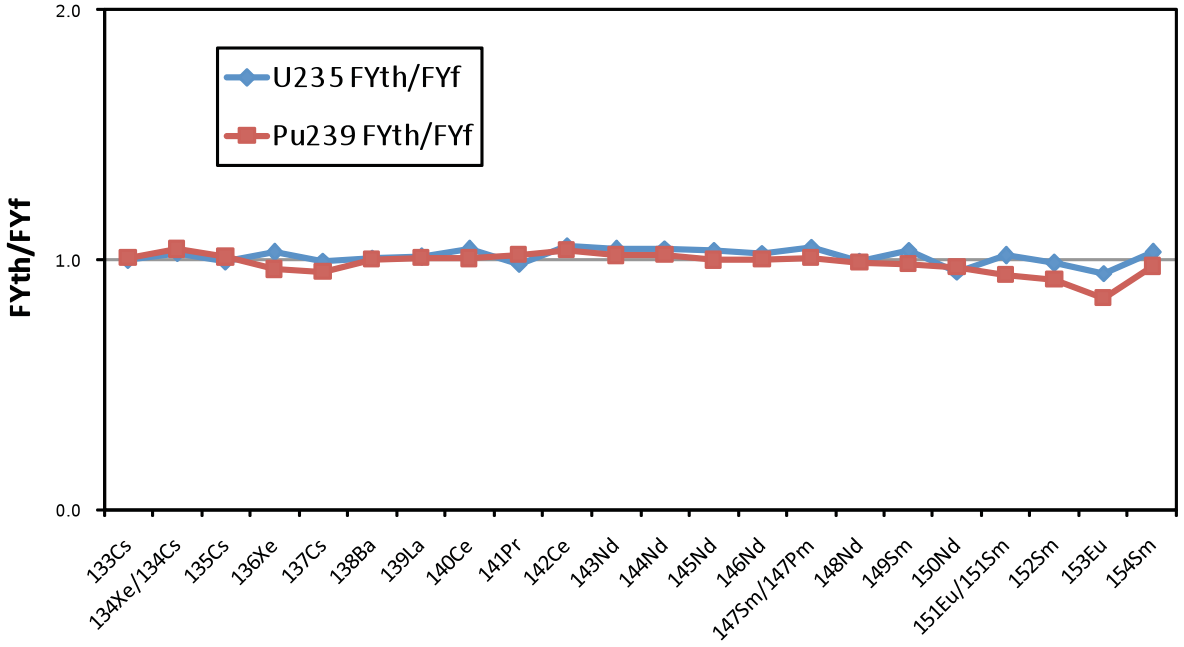

FigureB-5. Comparison of Cumulative Fission Yield between Thermal and Fast Injected Neutron Database (U-235 and Pu-239, ENDF/VII1).

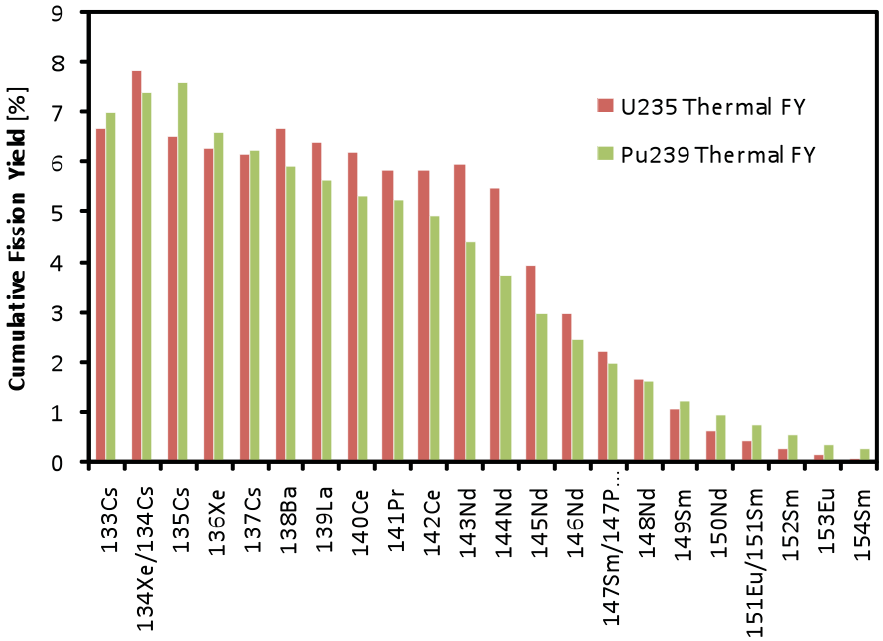

(a) Thermal Cumulative Fission Yield of REs

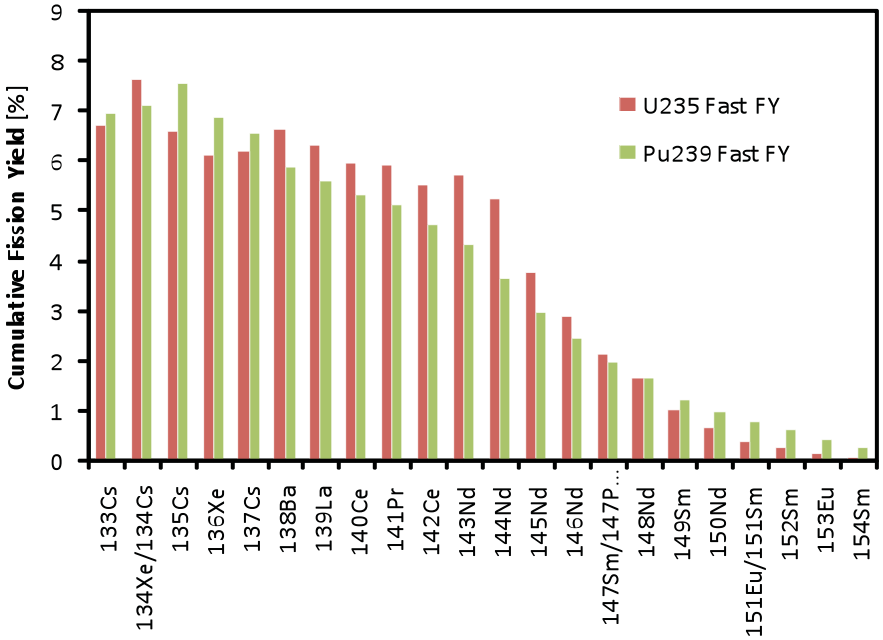

(b) Fast Cumulative Fission Yield REs

FigureB-6. Cumulative Fission Yield of U-235 and Pu-239 (ENDF/VII1).